Vectorial model for guided-mode resonance gratings

A.-L. Fehrembach,* B. Gralak, and A. Sentenac
Aix Marseille Univ, CNRS, Centrale Marseille, Institut Fresnel, Marseille, France

(Received 6 December 2017; revised manuscript received 5 February 2018; published 23 April 2018)

We propose a self-consistent vectorial method, based on a Green's function technique, to describe the resonances that appear in guided-mode resonance gratings. The model provides intuitive expressions of the reflectivity and transmittivity matrices of the structure, involving coupling integrals between the modes of a planar reference structure and radiative modes. When one mode is excited, the diffracted field for a suitable polarization can be written as the sum of a resonant and a nonresonant term, thus extending the intuitive approach used to explain the Fano shape of the resonance in scalar configurations. When two modes are excited, we derive a physical analysis in a configuration which requires a vectorial approach. We provide numerical validations of our model. From a technical point of view, we show how the Green's tensor of our planar reference structure can be expressed as two scalar Green's functions, and how to deal with the singularity of the Green's tensor.

DOI: 10.1103/PhysRevA.97.043852

I. INTRODUCTION

In photonics, resonant systems have stirred a growing interest for applications in filtering, chemical and biological sensing, light handling, harvesting, and absorption [1,2]. Among them, all-dielectric lossless guided-mode resonance gratings, made of a planar waveguide that is periodically structured, are particularly attractive for filtering applications [3,4]. Indeed, their resonance can be very narrow and, remarkably, the reflectivity and transmittivity can reach 100% provided that the structure satisfies appropriate symmetry conditions [5].

Depicting the spectrum of this structure with a simple model is of great interest, as an intuitive understanding facilitates the control of its properties (bandwidth, position, and amplitude). In this respect, the quasinormal-mode approach developed recently [6–10] brings a useful physical insight into the properties of resonant structures. In particular, these properties can be expressed in terms of coupling integrals involving the modes. Additional physical insight can be brought by perturbation theories, where the studied structure is seen as a reference structure whose eigenmodes are modified by a perturbation, leading to simple expressions of the modification of its properties [11]. This approach is particularly suitable for guided-mode resonance gratings, the reference structure being the planar waveguide (with normal modes) and the perturbation being the grating. Approximate models have been developed, based either on the coupled-mode method [12,13], very popular in the field of integrated optics, or on the Green's function formalism [14–16]. They have been helpful in the design of complex structures, such as the "biatomic grating," a solution to enhance the angular tolerance of the resonance [17,18].

Yet, most of them are restricted to the scalar problem [typically, a one-dimensional (1D) grating illuminated along a direction of periodicity], except Ref. [16] which solves the vectorial homogeneous problem. Now, the vectorial diffraction problem [1D grating illuminated under conical incidence, and two-dimensional (2D) grating] attracts strong interest, especially when polarization-independent configurations are sought [19–23]. The complexity of the behavior of resonant structures with respect to the incident polarization is then a strong incentive for developing a model giving a physical insight of the vectorial resonance phenomenon [24,25].

As demonstrated in Ref. [26], an efficient tool to study the behavior with respect to the incident polarization of any specularly diffracting structure is the set of eigenvalues of the reflectivity and transmittivity matrices in energy: they are the bounds of the reflectivity and transmittivity when the incident polarization takes any elliptical state. The associated eigenvectors correspond to the polarizations for which these bounds are reached. This approach is particularly powerful when the involved modes have nontrivial polarizations [24,25]. Yet, because the involved matrices contain both the resonant and the nonresonant parts of the diffracted field, the relation between the excited mode and the resonance of the eigenvalues is not intuitive. In this paper, we develop a vectorial approached model for guided-mode resonance gratings to provide this physical insight.

In Sec. II, we present the Green's tensor formalism to obtain a rigorous integral equation of the diffraction problem. Then, in Sec. III, we introduce the guided modes of a reference planar structure by expanding the Green's tensor on its eigenmodes. Making suitable assumptions, we obtain simplified expressions for the reflectivity and transmittivity matrices of the guided-mode resonance grating, involving coupling integrals between the guided modes and the radiative modes. In Sec. IV, we derive physical interpretations from these formulas, and provide numerical validations of our model. Our conclusion are presented in Sec. V. In the Appendices, we detail the calculation of the expansion of the Green's tensor, and provide additional numerical validations.

II. RIGOROUS INTEGRAL EQUATION

A. Geometry of the problem and notations

A Cartesian coordinate system (x,y,z) is used, with the unit vectors $\hat{\mathbf{x}}$, $\hat{\mathbf{y}}$, and $\hat{\mathbf{z}}$. As shown in Fig. 1(a), the structure

*Corresponding author: anne-laure.fehrembach@fresnel.fr

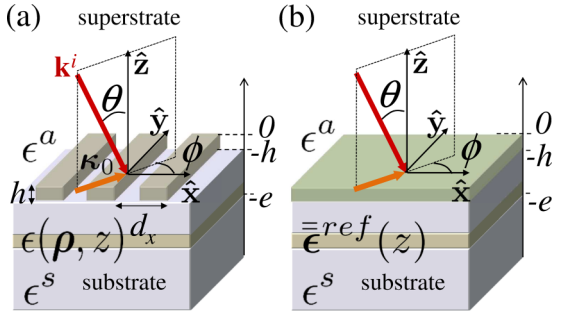

FIG. 1. (a) Studied configuration and notations. (b) Reference planar structure.

is composed of a stack of homogeneous layers of dielectric materials, which are supposed to be lossless and infinite along the x and y directions. A grating is engraved on top of the stack. The grating can be either periodic along the x direction only (1D grating) or along both the x and y directions (2D grating). The period along x and potentially y is denoted d_x and d_y, respectively. The grating pattern is composed of holes, the shape of which is invariant along the z direction between the planes defined by $z=-h$ and $z=0$. The relative permittivity of the studied structure is noted $\epsilon(\boldsymbol{\rho},z)$ with $\boldsymbol{\rho}=x\hat{\mathbf{x}}+y\hat{\mathbf{y}}$. It is equal to ϵ^a in the superstrate ($z>0$) and ϵ^s in the substrate ($z<-e$), where e is the total thickness of the stack, including the engraved layer and without the substrate and the superstrate, which are semi-infinite.

Throughout the paper, we consider harmonic fields with pulsation ω and wavelength in vacuum denoted λ, with temporal dependency $\exp(-i\omega t)$. The structure is illuminated with an incident plane wave coming from the superstrate. θ is the polar angle of incidence with respect to $\hat{\mathbf{z}}$, and ϕ is the azimuthal angle of incidence with respect to $\hat{\mathbf{x}}$ [see Fig. 1(a)]. The projection of the incident wave vector $\mathbf{k}^i$ on the (x,y) plane is denoted $\boldsymbol{\kappa}_0$. The projection, on the (x,y) plane, of the wave vector of the mth-order diffracted wave is

$$\boldsymbol{\kappa}_m=\boldsymbol{\kappa}_0+\mathbf{K}_m, \tag{1}$$

where $\mathbf{K}_m$ is the vector of the reciprocal space of the grating associated with the mth diffraction order. More precisely, for a grating periodic along the x direction only, $\mathbf{K}_m=m\frac{2\pi}{d_x}\hat{\mathbf{x}}$. For a grating periodic along both the x and y directions, the integer m is associated with the two relative integers labelling the (m_x,m_y) diffraction order and $\mathbf{K}_m=m_x\frac{2\pi}{d_x}\hat{\mathbf{x}}+m_y\frac{2\pi}{d_y}\hat{\mathbf{y}}$. The zero-diffraction order corresponds to $m=0$. Throughout the paper, we will consider configurations where the zero order is the only propagative order in the substrate and the superstrate.

For the sake of clarity, we consider structures containing a single grating, on top of the stack, and isotropic materials only. But the method can be easily extended to structures containing several gratings, whatever their location inside the stack, provided that the whole structure is still periodic, and also containing homogeneous anisotropic layers, with z symmetry axis.

B. Set of differential coupled equations

The electric field $\mathbf{E}$ is the solution of the equation

$$\boldsymbol{\nabla}\times\boldsymbol{\nabla}\times\mathbf{E}-k_0^2\epsilon\mathbf{E}=\mathbf{0}, \tag{2}$$

where $k_0=2\pi/\lambda$ is the wave number in vacuum. Since the structure is periodic along x and possibly y, the electric field is pseudoperiodic and can be written as a Floquet-Bloch expansion with coefficients $\mathbf{E}_m(z)$,

$$\mathbf{E}(\boldsymbol{\rho},z)=\sum_m\mathbf{E}_m(z)\exp(i\boldsymbol{\kappa}_\mathbf{m}\cdot\boldsymbol{\rho}). \tag{3}$$

We also expand the relative permittivity of the studied structure as a Fourier series, with coefficients $\epsilon_m(z)$,

$$\epsilon(\boldsymbol{\rho},z)=\sum_m\epsilon_m(z)\exp(i\mathbf{K}_\mathbf{m}\cdot\boldsymbol{\rho}). \tag{4}$$

Inserting Eqs. (3) and (4) into Eq. (2) leads to a set of differential equations coupling the diffraction orders,

$$\bar{\bar{\boldsymbol{\Omega}}}_m(\mathbf{E}_m(z))-k_0^2\sum_n\epsilon_{m-n}(z)\mathbf{E}_n(z)=\mathbf{0}, \tag{5}$$

where the operator $\bar{\bar{\boldsymbol{\Omega}}}_m$ is given by

$$\begin{aligned}\bar{\bar{\boldsymbol{\Omega}}}_m[\mathbf{E}_m(z)]=&\,i\boldsymbol{\kappa}_\mathbf{m}\times(i\boldsymbol{\kappa}_\mathbf{m}\times\mathbf{E}_m)+\hat{\mathbf{z}}\times\left(\hat{\mathbf{z}}\times\partial_z^2\mathbf{E}_m\right)\\&+(i\boldsymbol{\kappa}_m\cdot\partial_z\mathbf{E}_m)\hat{\mathbf{z}}+(\partial_z\mathbf{E}_m\cdot\hat{\mathbf{z}})i\boldsymbol{\kappa}_m.\end{aligned} \tag{6}$$

In the following paragraph, we derive an integral formulation from this equation, introducing the Green's tensor for a reference planar structure.

C. The reference problem

We consider a structure, called "reference structure," composed of the same homogeneous layers as the studied structure [see Fig. 1(b)]. In the grating region, to form the reference structure, the grating is replaced with a homogeneous layer with the same thickness, made of a material which can be anisotropic with symmetry axis z. This anisotropy yields a supplementary degree of freedom in the model without making the calculations too complex. The relative permittivity of the reference structure is denoted $\bar{\bar{\boldsymbol{\epsilon}}}^{\mathrm{ref}}$. We note ϵ^o as the permittivity in the (x,y) plane and ϵ^e along the z axis,

$$\bar{\bar{\boldsymbol{\epsilon}}}^{\mathrm{ref}}(z)=\epsilon^o(z)(\hat{\mathbf{x}}\hat{\mathbf{x}}+\hat{\mathbf{y}}\hat{\mathbf{y}})+\epsilon^e(z)\hat{\mathbf{z}}\hat{\mathbf{z}}. \tag{7}$$

Outside the grating region, $\epsilon^o(z)=\epsilon^e(z)=\epsilon(z)$, as the homogeneous materials of the studied structure are supposed to be isotropic. We will specify the expression of $\bar{\bar{\boldsymbol{\epsilon}}}^{\mathrm{ref}}$, depending on the relative permittivity of the grating, in Sec. II F.

We consider that the reference structure is illuminated with the same plane wave as the studied structure, with in-plane wave vector $\boldsymbol{\kappa}_0$ and wavelength λ. Hence, the field solution of the diffraction problem is $\mathbf{E}_0^{\mathrm{ref}}(z)\exp(i\boldsymbol{\kappa}_0.\boldsymbol{\rho})$, where $\mathbf{E}_0^{\mathrm{ref}}(z)$ is the solution of the following equation for $m=0$:

$$\bar{\bar{\boldsymbol{\Omega}}}_m\left[\mathbf{E}_m^{\mathrm{ref}}(z)\right]-k_0^2\bar{\bar{\boldsymbol{\epsilon}}}^{\mathrm{ref}}(z)\mathbf{E}_m^{\mathrm{ref}}(z)=\mathbf{0}. \tag{8}$$

On the other hand, a guided mode of the reference structure is expressed as $\mathbf{A}_m(z)\exp(i\boldsymbol{\kappa}_m\cdot\boldsymbol{\rho})$, where $\mathbf{A}_m(z)$ is solution of the homogeneous Eq. (8) for $m\neq0$ since the zero-diffraction order is propagating in the substrate and superstrate, while the guided modes must be evanescent in those media.

We now introduce the Green's tensor $\bar{\bar{\mathbf{G}}}_m(z,z')$, associated to the reference structure, as the solution of

$$\bar{\bar{\boldsymbol{\Omega}}}_m[\bar{\bar{\mathbf{G}}}_m(z,z')]-k_0^2\bar{\bar{\boldsymbol{\epsilon}}}^{\mathrm{ref}}(z)\bar{\bar{\mathbf{G}}}_m(z,z')=k_0^2\delta(z-z')\bar{\bar{\mathbf{I}}}, \tag{9}$$

and satisfying the outgoing wave condition. $\bar{\bar{\mathbf{I}}}$ is the identity tensor and $\delta(z-z')$ is the Dirac distribution. The index m indicates that the considered in-plane wave vector is $\boldsymbol{\kappa}_m$.

As the reference structure is anisotropic with symmetry axis z, Eqs. (8) and (9) can be expressed as two scalar problems for the two fundamental polarizations, i.e., transverse electric (TE) field and transverse magnetic (TM) field, with respect to the direction of propagation, as shown in Appendices A and B.

D. Rigorous integral equation

Once the Green's tensor solution of Eq. (9) is known, the differential equation (5) can be transformed into an integral equation. Equation (5) can be written as

$$\bar{\bar{\mathbf{\Omega}}}_m(\mathbf{E}_m) - k_0^2\bar{\bar{\boldsymbol{\epsilon}}}^{\mathrm{ref}}\mathbf{E}_m = k_0^2\sum_n[\epsilon_{m-n}\bar{\bar{\mathbf{I}}} - \delta_{m,n}\bar{\bar{\boldsymbol{\epsilon}}}^{\mathrm{ref}}]\mathbf{E}_n, \quad (10)$$

where $\delta_{m,n}$ is the Kronecker symbol. By subtracting Eq. (8) to Eq. (10), we obtain

$$\bar{\bar{\mathbf{\Omega}}}_m\left(\mathbf{E}_m^{\mathrm{pert}}\right) - k_0^2\bar{\bar{\boldsymbol{\epsilon}}}^{\mathrm{ref}}\mathbf{E}_m^{\mathrm{pert}} = k_0^2\sum_n\left[\epsilon_{m-n}\bar{\bar{\mathbf{I}}} - \delta_{m,n}\bar{\bar{\boldsymbol{\epsilon}}}^{\mathrm{ref}}\right]\mathbf{E}_n, \quad (11)$$

where we introduced the field $\mathbf{E}_m^{\mathrm{pert}}$ defined by

$$\mathbf{E}_m^{\mathrm{pert}} = \mathbf{E}_m - \mathbf{E}_m^{\mathrm{ref}}. \quad (12)$$

It has to be noted that since $\mathbf{E}_m$ and $\mathbf{E}_m^{\mathrm{ref}}$ are generated by the same incident field, $\mathbf{E}_m^{\mathrm{pert}}$ satisfies the outgoing wave condition. From Eq. (11), we deduce, using Eq. (9), that

$$\mathbf{E}_m(z) = \mathbf{E}_m^{\mathrm{ref}}(z) + \int_{-h}^{0} dz'\bar{\bar{\mathbf{G}}}_m(z,z')\sum_n[\epsilon_{m-n}(z')\bar{\bar{\mathbf{I}}} - \delta_{m,n}\bar{\bar{\boldsymbol{\epsilon}}}^{\mathrm{ref}}(z')]\mathbf{E}_n(z'), \quad (13)$$

where we used that the reference structure and the studied structure have the same permittivity outside the grating region (the grating region is for $z\in[-h,0]$). The calculation of the Green's tensor detailed in Appendix B shows that it presents a singularity on its $\hat{\mathbf{z}}\hat{\mathbf{z}}$ component (the same singularity as for layered isotropic materials [27]) and can be written as

$$\bar{\bar{\mathbf{G}}}_m(z,z') = \bar{\bar{\mathbf{G}}}_m^{\mathrm{NS}}(z,z') - \frac{1}{\epsilon^e}\delta(z-z')\hat{\mathbf{z}}\hat{\mathbf{z}}, \quad (14)$$

where $\bar{\bar{\mathbf{G}}}_m^{\mathrm{NS}}$ is the nonsingular part of $\bar{\bar{\mathbf{G}}}_m$. We show in the following paragraph how we can deal with this singularity.

E. Treatment of the singularity of the Green's tensor

The calculation of the integral over z of the singularity in Eq. (13) leads to the term

$$-\frac{\hat{\mathbf{z}}\hat{\mathbf{z}}}{\epsilon^e}\sum_n[\epsilon_{m-n}(z)\bar{\bar{\mathbf{I}}} - \delta_{m,n}\bar{\bar{\boldsymbol{\epsilon}}}^{\mathrm{ref}}(z)]\mathbf{E}_n(z). \quad (15)$$

By transferring this term to the left-hand side of Eq. (13), we can write

$$\mathbf{F}_m(z) = \mathbf{E}_m^{\mathrm{ref}}(z) + \int_{-h}^{0} dz'\bar{\bar{\mathbf{G}}}_m^{\mathrm{NS}}(z,z')\sum_n[\epsilon_{m-n}(z')\bar{\bar{\mathbf{I}}} - \delta_{m,n}\bar{\bar{\boldsymbol{\epsilon}}}^{\mathrm{ref}}(z')]\mathbf{E}_n(z'), \quad (16)$$

where

$$\mathbf{F}_m(z) = \sum_n\left[\delta_{m,n}(\hat{\mathbf{x}}\hat{\mathbf{x}}+\hat{\mathbf{y}}\hat{\mathbf{y}}) + \frac{\epsilon_{m-n}(z)}{\epsilon^e(z)}\hat{\mathbf{z}}\hat{\mathbf{z}}\right]\mathbf{E}_n(z). \quad (17)$$

From Eq. (17), we can express $\mathbf{E}_n$ as a function of $\mathbf{F}_m$,

$$\mathbf{E}_n(z) = \sum_m\left\{\delta_{m,n}(\hat{\mathbf{x}}\hat{\mathbf{x}}+\hat{\mathbf{y}}\hat{\mathbf{y}}) + \epsilon^e(z)\left[\frac{1}{\epsilon(z)}\right]_{n-m}\hat{\mathbf{z}}\hat{\mathbf{z}}\right\}\mathbf{F}_m(z), \quad (18)$$

where $\left[\frac{1}{\epsilon(z)}\right]_p$ is the pth coefficient of the Fourier expansion of the function $1/\epsilon(z)$. Last, by replacing $\mathbf{E}_n$ with this expression into Eq. (16), we obtain

$$\mathbf{F}_m(z) = \mathbf{E}_m^{\mathrm{ref}}(z) + \int_{-h}^{0} dz'\bar{\bar{\mathbf{G}}}_m^{\mathrm{NS}}(z,z')\sum_n\bar{\bar{\boldsymbol{\xi}}}_{m-n}(z')\mathbf{F}_n(z'), \quad (19)$$

where $\bar{\bar{\boldsymbol{\xi}}}_{m-n}(z)$ is defined by

$$\bar{\bar{\boldsymbol{\xi}}}_{m-n}(z) = [\epsilon_{m-n}(z) - \epsilon^o(z)\delta_{m,n}](\hat{\mathbf{x}}\hat{\mathbf{x}}+\hat{\mathbf{y}}\hat{\mathbf{y}}) + \epsilon^e(z)\left\{\delta_{m,n} - \epsilon^e(z)\left[\frac{1}{\epsilon(z)}\right]_{m-n}\right\}(\hat{\mathbf{z}}\hat{\mathbf{z}}), \quad (20)$$

taking into account that $\sum_p[\epsilon]_{m-p}\left[\frac{1}{\epsilon}\right]_{p-n} = \delta_{m,n}$. It is useful to note that $\mathbf{F}_m$ is equal to $\mathbf{E}_m$ outside the grating region. In the grating region, they differ only for the $\hat{\mathbf{z}}$ component. Equation (19) represents the coupling between the mth order and the nth order, through the coefficient $\bar{\bar{\boldsymbol{\xi}}}_{m-n}$, representing the perturbation induced by the grating on the reference structure.

F. Choice of the reference structure

We choose the planar reference structure such that it gives a diffracted field as close as possible to the field diffracted by the considered structure. In other words, the perturbation, represented by the coefficients $\bar{\bar{\boldsymbol{\xi}}}_p$, must not allow the direct coupling from one order to itself. This condition mathematically translates into $\bar{\bar{\boldsymbol{\xi}}}_0 = 0$. From the expression of $\bar{\bar{\boldsymbol{\xi}}}_{m-n}$ [Eq. (20)], we deduce that

$$\epsilon^o = \epsilon_m\delta_{m,0} \quad \text{and} \quad \epsilon^e = \left[\frac{1}{\epsilon(z)}\right]_m^{-1}\delta_{m,0}. \quad (21)$$

Hence, the ordinary permittivity ϵ^o must be equal to the geometric average of the grating permittivity, and the extraordinary permittivity ϵ^e must be equal to its harmonic average. First of all, note that this result directly follows from our hypothesis for the reference structure to be anisotropic with the z axis. It also comes from the fact that we first performed a Fourier transform in the (x,y) plane, leading to a perturbative model with respect to the grating depth h [see Eq. (19)], and to a homogenization of the grating in the limit of small depths. As a matter of fact, the singularity of our Green's tensor is the same as the singularity calculated by Yaghjian [28] when integrating the Green's tensor of a homogeneous medium in the source region over a thin "pillar box" in the (x,y) plane. Moreover, our result is consistent with the well-known rules for the homogenization of a periodic assembly of thin plates [29]: the effective permittivity is the geometric average of the permittivities for

the directions where the electric field is continuous through the plates' interfaces (i.e., directions parallel to the plane of the plates), while it is the harmonic average for the direction where the electric displacement is continuous (i.e., direction perpendicular to the plane of the plates). Usually, the plates are parallel to each others [29], e.g., the direction of periodicity is perpendicular to the plane of the plates. Our case differs since our plates are juxtaposed in the (x,y) plane, e.g., the directions of periodicity are contained in the plane of the plates. Yet, the same rules apply: the direction of the plates imposes the form of the permittivity tensor, while the directions of periodicity give the directions along which the average is performed. The rule of the geometric average in the plane for a small-depth 1D or 2D grating was already mentioned in Ref. [30]. Last, one could expect that the z-axis anisotropic reference structure is more suitable to model 2D gratings (with $\pi/2$ rotation invariance around z) than 1D gratings, as the latter creates a strong-form anisotropy in the (x,y) plane. Yet, it is important to note that the excited guided modes propagate in directions close to the directions of periodicity of the grating (due to the coupling condition). As a consequence, the fact that the 1D grating has a translation invariance along its ridges has a minor impact on the propagation of the guided mode. Hence, the model has the same accuracy for 1D and 2D gratings, as will be shown by the numerical calculations.

It must be noted that Eq. (19) is rigorous. We will now make approximations in order to obtain an expression of the diffracted field.

III. APPROACHED EXPRESSION OF THE DIFFRACTED FIELD

We consider that the angles of incidence are fixed, and we are interested in deriving an expression of the diffracted field with respect to the wavelength. We suppose that the reference structure supports guided modes in the range of the considered wavelengths and that these eigenmodes can be excited through diffraction orders of the grating (except the zero order). The coupling condition can be satisfied when the in-plane wave vector of a diffraction order ($\boldsymbol{\kappa}_q$) has its modulus close to the propagation constant of a guided mode. We note $\mathcal{Q}$ as the set of integers q corresponding to the resonant diffraction orders. Depending on the configuration, $\mathcal{Q}$ can contain only one or several integers. In the following, we treat the general case where $\mathcal{Q}$ contains several integers, the case of a single resonant order being easily deduced from this general case.

A. Eigenmodes of the Green's tensor

As detailed in Appendix D, based on results demonstrated in Appendix C, the regular part of the Green's tensor for our planar reference structure can be expanded on the basis of its eigenmodes. As a first simplifying hypothesis, we suppose that in the vicinity of the resonance wavelength of one mode, the term corresponding to this mode prevails over the other terms of the sum. Hence, for a resonant order $q \in \mathcal{Q}$, we write, in the vicinity of the resonance wavelength λ_q of the excited mode,

$$\bar{\bar{\mathbf{G}}}_q^{\mathrm{NS}}(z,z') \simeq \frac{\mathbf{A}_q(z) \otimes \overline{\mathbf{A}_q}(z')}{\left[\left(\frac{\lambda}{\lambda_q}\right)^2 - 1\right]}, \tag{22}$$

where $\otimes$ denotes the tensor product between two vectors, $\mathbf{A}_q$ is the electric field of the excited guided mode of the reference structure, and $\overline{\mathbf{A}_q}$ is its complex conjugated. This mode is the solution of the homogeneous problem associated with Eq. (8) for $m = q$. In the following, we will consider that λ is always different from any λ_q. Hence, the only non-null component of the reference field in Eq. (19) is $\mathbf{E}_0^{\mathrm{ref}}(z)$.

B. Approached integral equations

The Green's tensor $\bar{\bar{\mathbf{G}}}_q^{\mathrm{NS}}$ appears as a common factor in the sum contained in the expression of the diffraction order $\mathbf{F}_q$ given by Eq. (19). Injecting Eq. (22) into Eq. (19) for $m = q \in \mathcal{Q}$, we obtain

$$\mathbf{F}_q(z) \simeq \frac{\mathbf{A}_q(z)}{\left[\left(\frac{\lambda}{\lambda_q}\right)^2 - 1\right]} \int_0^{-h} dz' \overline{\mathbf{A}_q}(z') \cdot \left[\sum_{n \notin \mathcal{Q}} \bar{\bar{\boldsymbol{\xi}}}_{q-n}(z') \mathbf{F}_n(z') + \sum_{q' \in \mathcal{Q}} \bar{\bar{\boldsymbol{\xi}}}_{q-q'}(z') \mathbf{F}_{q'}(z') \right], \tag{23}$$

where we have considered that $q \neq 0$ and separated the sums of the resonant and the nonresonant terms. Note that the tensor product $\otimes$ is no longer necessary in this equation since the quantity under the integral is scalar [scalar product between the vector $\overline{\mathbf{A}_q}(z')$ and the vector in the brackets]. We can expect that in the vicinity of λ_q, the resonant orders $\mathbf{F}_q$ are predominant over the nonresonant orders. Hence, in the sum contained in the expression of a nonresonant order $\mathbf{F}_n$ for $n \notin \mathcal{Q}$, we retain only the resonant orders, as a second simplifying hypothesis:

$$\mathbf{F}_n(z) \simeq \mathbf{E}_0^{\mathrm{ref}}(z)\delta_{n,0} + \int_{-h}^{0} dz' \bar{\bar{\mathbf{G}}}_n^{\mathrm{NS}}(z,z') \sum_{q \in \mathcal{Q}} \bar{\bar{\boldsymbol{\xi}}}_{n-q}(z') \mathbf{F}_q(z'). \tag{24}$$

Once the $\mathbf{F}_q$ are calculated (see the next paragraph), Eq. (24) will be used to express the field diffracted in the nonresonant orders, and especially the zero order.

C. Coupling integrals

The third simplifying hypothesis is to consider that the field in a resonant order q is proportional to the field of the guided mode $\mathbf{A}_q$ (as in [14]),

$$\mathbf{F}_q = \sigma_q \mathbf{A}_q, \tag{25}$$

with σ_q as proportionality coefficient. This hypothesis is suggested by the form of Eq. (23), where $\mathbf{A}_q(z)$ appears as a factor. One could be tempted to write that $\mathbf{F}_q$ is proportional to $\frac{\mathbf{A}_q(z)}{[(\frac{\lambda}{\lambda_q})^2-1,]}$. Yet, note that the eigenwavelength of the modes of the studied structure is different from that of the planar reference structure, and hence λ_q cannot be a pole of $\mathbf{F}_q$. In particular, the modes of the structure perturbed by the grating are leaky modes. This means that their eigenwavelengths are complex numbers [31].

Injecting Eq. (25) into Eq. (24) leads to

$$\mathbf{F}_n(z) \simeq \mathbf{E}_0^{\mathrm{ref}}(z)\delta_{n,0} + \sum_{q \in \mathcal{Q}} \sigma_q \boldsymbol{\Gamma}_{n,q}(z), \tag{26}$$

where $\mathbf{\Gamma}_{n,q}(z)$ is a vector corresponding to the outcoupling out of the mode q through the nth-diffraction order,

$$\mathbf{\Gamma}_{n,q}(z) = \int_{-h}^{0} dz' \bar{\bar{\mathbf{G}}}_n^{\mathrm{NS}}(z,z') \bar{\bar{\boldsymbol{\xi}}}_{n-q}(z') \mathbf{A}_q(z'). \tag{27}$$

In order to calculate the σ_q coefficients, we report the expression of $\mathbf{F}_n$ given by Eq. (24) into Eq. (23), and use the proportionality relation [Eq. (25)]. We obtain

$$\mathbf{F}_q(z) \simeq \frac{\mathbf{A}_q(z)}{\left[\left(\frac{\lambda}{\lambda_q}\right)^2 - 1\right]} \left[C_{q,0} + \sum_{q' \in \mathcal{Q}} \sigma_{q'} \left(C_{q,q'} + \sum_{n \notin \mathcal{Q}} C_{q,n,q'} \right) \right], \tag{28}$$

where we introduced the following:

(i) the coupling integral between the reference field and the mode (excitation of the mode),

$$C_{q,0} = \int_{-h}^{0} dz' \overline{\mathbf{A}_q}(z') \bar{\bar{\boldsymbol{\xi}}}_q(z') \mathbf{E}_0^{\mathrm{ref}}(z'), \tag{29}$$

(ii) the direct coupling integral between the mode q and the mode q',

$$C_{q,q'} = \int_{-h}^{0} dz' \overline{\mathbf{A}_q}(z') \bar{\bar{\boldsymbol{\xi}}}_{q-q'}(z') \mathbf{A}_{q'}(z'), \tag{30}$$

(iii) the second-order coupling integral between the mode q and the mode q' through the nth order,

$$C_{q,n,q'} = \int_{-h}^{0} dz' \overline{\mathbf{A}_q}(z') \bar{\bar{\boldsymbol{\xi}}}_{q-n}(z') \int_{-h}^{0} dz'' \bar{\bar{\mathbf{G}}}_n^{\mathrm{NS}}(z',z'') \times \bar{\bar{\boldsymbol{\xi}}}_{n-q'}(z'') \mathbf{A}_{q'}(z''). \tag{31}$$

Last, from Eq. (28), we find that the coefficients σ_q are the solutions of the system of linear equations,

$$\sigma_q \left[\left(\frac{\lambda}{\lambda_q}\right)^2 - 1 - \Sigma_{q,q} \right] - \sum_{q' \in \mathcal{Q}} \sigma_{q'} (C_{q,q'} + \Sigma_{q,q'}) = C_{q,0}, \tag{32}$$

where we introduced the notation $\Sigma_{q,q'} = \sum_{n \notin \mathcal{Q}} C_{q,n,q'}$. This system of equations shows how the coefficients σ_q are modified by the direct coupling between the modes and also by the second-order coupling, which appears in Eq. (32) as the sum of the integrals $C_{q,n,q'}$. Numerically, we will calculate this sum for n from $-N$ to N, and consider N as a convergence parameter.

We represented in Fig. 2 a sketch illustrating the couplings, through the coupling integrals [Eqs. (27) and (29)–(31)], in the case of one resonant order only [Fig. 2(a)] and two resonant orders [Fig. 2(b)].

D. Reflection and transmission matrices

To express the reflection and transmission matrices of the structure (for the zero-diffraction order only), we introduce the basis related to the s and p polarizations. To each diffraction order m, we associate the vector $\hat{\mathbf{s}}_m = \hat{\boldsymbol{\kappa}}_m \times \hat{\mathbf{z}}$. Moreover, for the incident, reflected, and transmitted plane waves with wave vectors $\mathbf{k}^i$, $\mathbf{k}^r$, and $\mathbf{k}^t$, respectively, we introduce the vectors $\hat{\mathbf{p}}^i = \hat{\mathbf{s}}_0 \times \hat{\mathbf{k}}^i$, $\hat{\mathbf{p}}^r = \hat{\mathbf{s}}_0 \times \hat{\mathbf{k}}^r$, and $\hat{\mathbf{p}}^t = \hat{\mathbf{s}}_0 \times \hat{\mathbf{k}}^t$ (see Fig. 3).

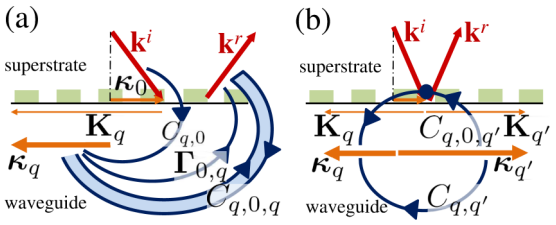

FIG. 2. Sketch of the coupling integrals. (a) One resonant order q: excitation of the mode ($C_{q,0}$), outcoupling ($\mathbf{\Gamma}_{0,q}$), and second-order self-coupling through the zero order ($C_{q,0,q}$). (b) Two resonant orders q and q': direct coupling between the two modes ($C_{q,q'}$) and second-order coupling through the zero order ($C_{q,0,q'}$).

The reflection and transmission coefficients can be deduced from Eq. (26) for $n = 0$. Indeed, since the field $\mathbf{F}_n$ is equal to $\mathbf{E}_n$ outside the grating region, Eq. (26) writes, for $z > 0$ and $z < -h$,

$$\mathbf{E}_0(z) \simeq \mathbf{E}_0^{\mathrm{ref}}(z)\delta_{n,0} + \sum_{q \in \mathcal{Q}} \sigma_q \mathbf{\Gamma}_{0,q}(z). \tag{33}$$

For $z > 0$, the reference field $\mathbf{E}_0^{\mathrm{ref}}(z)$ is the sum of the incident field with amplitude $\mathbf{E}_0^{\mathrm{inc}}$ and the field reflected by the reference structure, with amplitude $\mathbf{E}_0^{\mathrm{ref},r}$,

$$\mathbf{E}_0^{\mathrm{ref}}(z) = \mathbf{E}_0^{\mathrm{inc}} \exp(-i\gamma_a z) + \mathbf{E}_0^{\mathrm{ref},r} \exp(i\gamma_a z), \tag{34}$$

where $\gamma_a = \sqrt{\epsilon^a k_0^2 - \kappa_0^2}$. For $z > 0$, the Green's tensor $\bar{\bar{\mathbf{G}}}_0^{\mathrm{NS}}(z,z')$ can be written as $\bar{\bar{\mathbf{G}}}_0^{\mathrm{NS}}(0,z')\exp(i\gamma_a z)$, and hence

$$\mathbf{\Gamma}_{0,q}(z) = \exp(i\gamma_a z) \int_{-h}^{0} dz' \bar{\bar{\mathbf{G}}}_0^{\mathrm{NS}}(0,z') \bar{\bar{\boldsymbol{\xi}}}_{-q}(z') \mathbf{A}_q(z'). \tag{35}$$

Taking into account these remarks, we obtain the field $\mathbf{E}_0^r(z)$ (for $z > 0$) reflected by the studied structure in the zero order,

$$\mathbf{E}_0^r(z) \simeq \left[\mathbf{E}_0^{\mathrm{ref},r} + \sum_{q \in \mathcal{Q}} \sigma_q \mathbf{\Gamma}_{0,q}(0) \right] \exp(i\gamma_a z). \tag{36}$$

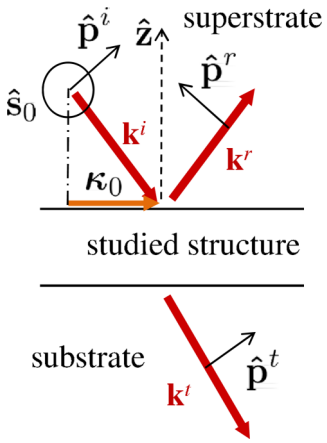

FIG. 3. The (s,p) basis associated with the propagative diffraction orders.

The vector $\mathbf{\Gamma}_{0,q}(0)$ represents the electric field of the mode in the diffraction order q coupled out by the grating through the zero order. Its components in the (s,p) basis are denoted $C^s_{0,q} = \mathbf{\Gamma}_{0,q}(0)\cdot\hat{\mathbf{s}}_0$ and $C^p_{0,q} = \mathbf{\Gamma}_{0,q}(0)\cdot\hat{\mathbf{p}}^r$.

Now, we consider successively a s- and a p-polarized incident field, and denote σ^s_q and σ^p_q the solutions calculated from Eq. (32) by considering, respectively, a s and a p incident field in $C_{q,0}$ [Eq. (29)]. We deduce from Eq. (36) an approached expression of the reflectivity matrix $\mathbf{R}$ (zero-diffraction order only) of the structure in the (s,p) basis,

$$\mathbf{R} \simeq \mathbf{R}^{\text{ref}} + \sum_{q\in\mathcal{Q}} \mathbf{R}^{\text{pert}}_q. \tag{37}$$

The 2×2 matrices $\mathbf{R}$ and $\mathbf{R}^{\text{ref}}$ contain the reflectivity coefficients for the studied structure and reference structure, respectively, expressed in the (s,p) basis, and the $\mathbf{R}^{\text{pert}}_q$ matrices are given by

$$\mathbf{R}^{\text{pert}}_q = \begin{bmatrix} \sigma^s_q C^s_{0,q}(0) & \sigma^p_q C^s_{0,q}(0) \\ \sigma^s_q C^p_{0,q}(0) & \sigma^p_q C^p_{0,q}(0) \end{bmatrix}. \tag{38}$$

Following the same steps for $z<-e$, we obtain an approached expression of the transmittivity matrix $\mathbf{T}$ (zero-diffraction order only) of the structure

$$\mathbf{T} = \mathbf{T}^{\text{ref}} + \sum_{q\in\mathcal{Q}} \mathbf{T}^{\text{pert}}_q, \tag{39}$$

where $\mathbf{T}$ and $\mathbf{T}^{\text{ref}}$ are 2×2 matrices containing the transmittivity coefficients for the studied structure and reference structure, respectively, expressed in the (s,p) basis, and

$$\mathbf{T}^{\text{pert}}_q \simeq \begin{bmatrix} \sigma^s_q C^s_{0,q}(-e) & \sigma^p_q C^s_{0,q}(-e) \\ \sigma^s_q C^p_{0,q}(-e) & \sigma^p_q C^p_{0,q}(-e) \end{bmatrix}. \tag{40}$$

Equations (37) and (39) are intuitive expressions of the reflectivity and transmittivity matrices of a guided-mode resonance grating, where the coupling in and out of a mode appears as an additional term to the reflectivity and transmittivity matrices of a reference structure. In other words, the field reflected and transmitted by the structure is described by the interference of a resonant term ($\mathbf{R}^{\text{pert}}_q$ and $\mathbf{T}^{\text{pert}}_q$) and a nonresonant term ($\mathbf{R}^{\text{ref}}$ and $\mathbf{T}^{\text{ref}}$). These expressions are the vectorial counterparts of the scalar expressions for the reflectivity and transmittivity coefficients that are used to explain the Fano resonance appearance of the guided-mode resonances in configurations where the polarization of the field reflected and transmitted is the same as that of the incident field [32]. The vectorial expressions must be used in the more complex and general case of configurations where the polarization of the resonant field is not the same as the polarization of the nonresonant field. This result is represented by a sketch in Fig. 4. The addition is expressed in terms of coupling integrals involving the excited modes and radiative modes. The present formulation takes into account the effect of the polarization (of the incident field and of the field diffracted by the studied structure, as well as that of the mode). We believe in the usefulness of the vectorial formulation since the behavior of guided-mode resonance gratings with respect to the incident polarization may in some configurations be surprising [24,25].

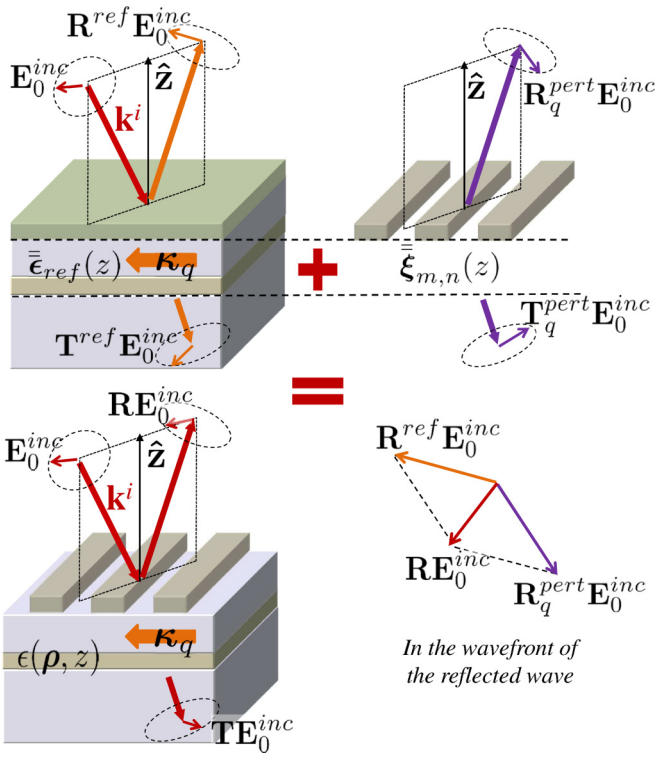

FIG. 4. At resonance, the reflected and transmitted fields are the sum of a nonresonant term, coming from the planar reference structure, and a resonant term, which is due to the grating. The vectorial sum of the field in the wavefront of the reflected wave is represented on the right bottom sketch.

IV. PHYSICAL ANALYSIS AND NUMERICAL VERIFICATIONS

We will consider successively the two situations where first only one order is resonant and then two orders are resonant. The former situation corresponds to the general case of oblique incidence. The latter situation will be reduced to the particular case where the plane of incidence is a plane of symmetry of the structure (full conical incidence). Particular attention will be paid to the influence of the incident polarization. For the validation of the model, we compare the results to the reflection and transmission coefficients calculated with a homemade code based on the rigorous Fourier modal method [33], which has been thoroughly validated by comparison with other codes [34] and experiments [23]. We tested the convergence with respect to the number N of coefficients taken in the sum on the nonresonant orders of Eq. (32) ($\Sigma_{q,q'} = \sum_{n(\notin\mathcal{Q})=-N}^{N} C_{q,n,q'}$).

A. Situation with one resonant order only

In the situation where only one order is resonant, the system [Eq. (32)] reduces to the single equation

$$\sigma_q = \frac{C_{q,0}}{\left[\left(\frac{\lambda}{\lambda_q}\right)^2 - 1 - \Sigma_{q,q}\right]}, \tag{41}$$

from which the eigenwavelength λ_q^{pert} of the mode of the studied structure can be deduced (this is the pole of σ_q),

$$\lambda_q^{\text{pert}} = \lambda_q \sqrt{1 + \Sigma_{q,q}}, \tag{42}$$

and appears as a modification of the eigenwavelength of the excited eigenmode caused by the second-order self-coupling of the mode through the diffraction orders. Let us note that the imaginary part of this pole gives the half width of the resonance peak. As λ_q is real, the width of the peak depends on the second-order coupling coefficients $C_{q,n,q}$, and depicts the leakage in the substrate and the superstrate of the excited mode. As we consider that the zero-diffraction order is the only propagative one, we can expect that the width of the resonance peak is mainly given by $C_{q,0,q}$, and that $C_{q,n,q}$ for $n \neq 0$ plays a minor role. $C_{q,0,q}$ includes the qth harmonic of the permittivity of the grating, as was already underlined in the literature concerning guided-mode resonance gratings [12,14,15,17].

Further, an important property can be easily derived from the expression of $\mathbf{R}_q^{\text{pert}}$ [see Eq. (38)], which is valid even when several orders are resonant. The determinant of $\mathbf{R}_q^{\text{pert}}$ is null, and hence one eigenvalue of $\mathbf{R}_q^{\text{pert}}$ is null and the other, called μ_q, is equal to the trace of $\mathbf{R}_q^{\text{pert}}$,

$$\mu_q = \sigma_q^s C_{0,q}^s(0) + \sigma_q^p C_{0,q}^p(0). \tag{43}$$

The eigenvector associated with μ_q is $\mathbf{V} = [C_{0,q}^s(0); C_{0,q}^p(0)]$. The eigenvector associated with the null eigenvalue is $\mathbf{V}_0 = [\sigma_q^p; -\sigma_q^s]$. Similar properties can be derived for the transmission matrix.

Now, in the particular case where only one order q is resonant, the non-null eigenvalue of $\mathbf{R}_q^{\text{pert}}$ takes the form

$$\mu_q = \frac{\left[C_{q,0}^s C_{0,q}^s(0) + C_{q,0}^p C_{0,q}^p(0)\right]}{\left[\left(\frac{\lambda}{\lambda_q}\right)^2 - 1 - \Sigma_{q,q}\right]}, \tag{44}$$

where $C_{q,0}^s$ and $C_{q,0}^p$ are obtained by considering, respectively, a s and a p incident field in $C_{q,0}$ [Eq. (29)].

Note that the incident polarization corresponding to the eigenvector $\mathbf{V}$ associated with μ_q may not be the one giving the maximum reflectivity, since the reflectivity of the reference structure must also be taken into account [see Eq. (37) and the right bottom sketch in Fig. 4]. For further physical analysis, it is useful to calculate the reflected field when the incident wave is colinear to $\mathbf{V}$ (eigenvector associated with the resonant eigenvalue). We obtain, for the reflected field along $\mathbf{V}$,

$$\mu_q + \frac{r_s C_{q,0}^s C_{0,q}^s(0) + r_p C_{q,0}^p C_{0,q}^p(0)}{C_{q,0}^s C_{0,q}^s(0) + C_{q,0}^p C_{0,q}^p(0)}, \tag{45}$$

where r_s and r_p are the reflection coefficients of the reference structure for s and p polarization, respectively. The reflected field along $\mathbf{V}_0$ (eigenvector associated with the null eigenvalue) is

$$\frac{(r_s - r_p) C_{0,q}^s(0) C_{0,q}^p(0)}{\mu_q}. \tag{46}$$

First of all, it appears that the component along $\mathbf{V}$ is resonant for a wavelength close to λ_q [see Eq. (43)], while the component along $\mathbf{V}_0$ vanishes for the same wavelength. Thus, when the mode is excited with the suitable polarization, the field is reflected without polarization change. Second, the component along $\mathbf{V}$ is the sum of a resonant term and a nonresonant term. Taking λ close to λ_q, the resonant denominator of μ_q can be simplified as $(\frac{\lambda}{\lambda_q})^2 - 1 - \Sigma_{q,q} \simeq 2[(\frac{\lambda}{\lambda_q}) - 1] - \Sigma_{q,q}$ to bring out the Fano-shape appearance of the resonance, with centering wavelength λ_q and width equal to the imaginary part of $\Sigma_{q,q}$. In particular, in the classical configuration where the grating is illuminated along one direction of periodicity and a TE mode is excited with s incident polarization, $C_{q,0}^p C_{0,q}^p(0)$ vanishes and one retrieves the simple intuitive formula used to describe the Fano resonance in the scalar case [32], with the reflectivity of the planar structure as the nonresonant term. Similar comments hold for a TM mode excited with p polarization. In the general case of conical incidence, both the coupling in and out of the mode and the nonresonant reflectivity are a mixture of the s and p components. Last, it is possible to show that the term $(\frac{\lambda}{\lambda_q})^2 - 1 - \Sigma_{q,q}$ is not present in the expression of the field reflected when the incident wave is colinear to the eigenvector $\mathbf{V}_0$. The resonance does not appear for this polarization.

To validate our model and our conclusions in the case where only one order is resonant, we consider the configuration 1 involving a TM mode, a 1D grating, and conical incidence. The structure of this configuration 1 is composed of a substrate with a dielectric permittivity of 2.097, a first layer with a 301.2 nm thickness and a 4.285 permittivity, a second layer with a 140.4 nm thickness and a 2.161 permittivity, a grating with depth 70 nm, period 838 nm, grooves width 300 nm engraved in a 2.161 permittivity material and filled with air (permittivity 1). The superstrate is also air. The angles of incidence are $\theta = 15^\circ$ and $\phi = 50.5^\circ$ (see Fig. 1 for the definition of θ and ϕ). In this configuration, a TM guided mode is excited around 1.459 μm, and under conical incidence through the -1 diffraction order. The resonance is observable for both s (incident electric field perpendicular to the plane of incidence) and p (incident magnetic field perpendicular to the plane of incidence) polarizations.

We compare in Fig. 5(a), for s incident polarization, and Fig. 5(b), for p polarization, the reflectivity and transmittivity calculated with the approached method for $N = 10$ (dashed lines, R and T) and with the rigorous method (solid lines, Rrig and Trig). We also plot the reflectivity and transmittivity for the reference planar structure (dotted lines, Rref and Tref) and the sum of the reflectivity and transmittivity calculated with the approached method (dashed green line, R+T).

First, we observe that the resonance is well depicted, with a resonance wavelength, as well as a width and maxima close to the rigorous ones, both for s and p polarizations, for the transmission and the reflection. We also observe that R+T is close to 1, i.e., the energy conservation is satisfied. Last, we observe that the reflectivity and transmittivity of the studied structure tend to that of the unperturbed structure far from the resonance.

In Fig. 5(c), we plot the reflectivity at resonance for any linear polarization with respect to the angle between the electric incident field and the s polarization, both for the rigorous and the approached calculation. As expected from the analysis of the previous paragraph in the case of one resonant order

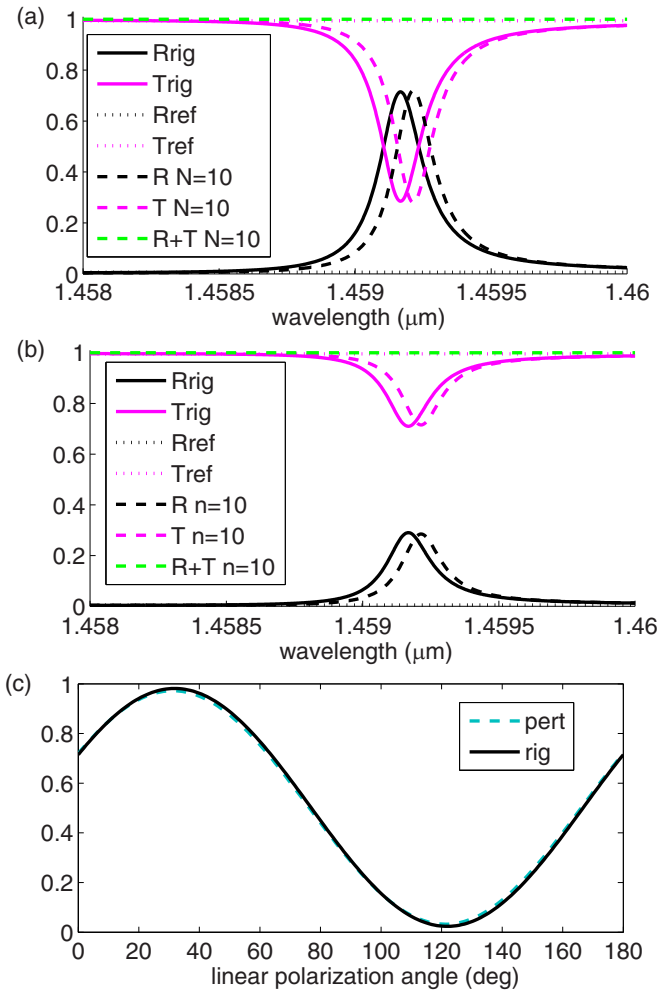

FIG. 5. Configuration 1—Reflectivity and transmittivity spectra calculated rigorously (straight lines, Rrig and Trig), with the approached method for $N = 10$ (dashed lines, R and T, and sum R+T) and for the reference structure (dotted lines, Rref and Tref): (a) for the s incident polarization and (b) for the p polarization. (c) Reflectivity at resonance for any linear polarization with respect to the angle between the electric field and the s polarization, calculated with the approached method for $N = 10$ (dotted cyan line) and rigorously (black straight line).

only, we have a polarization (quasilinear polarization with an angle 31.7° with the s polarization) for which the mode is fully excited, and not at all for the orthogonal polarization (quasilinear polarization with an angle 121.7°).

To study the impact of the number of orders taken when summing the coefficients $C_{q,n,q'}$ for n from $-N$ to N, we plot in Fig. 6(a) the resonance wavelength calculated with the approached model for various values of N, and the resonance wavelength calculated rigorously, for comparison. The spectra for some values of N are plotted in Fig. 6(b). We observe that the peak calculated with the approached method is positioned at a shorter wavelength than the peak calculated rigorously when $N = 0$, and it moves to higher wavelengths when N grows. The final difference is no more than a quarter of the bandwidth of the peak. As expected, the width of the peak is not much modified with respect to that obtained for $N = 0$.

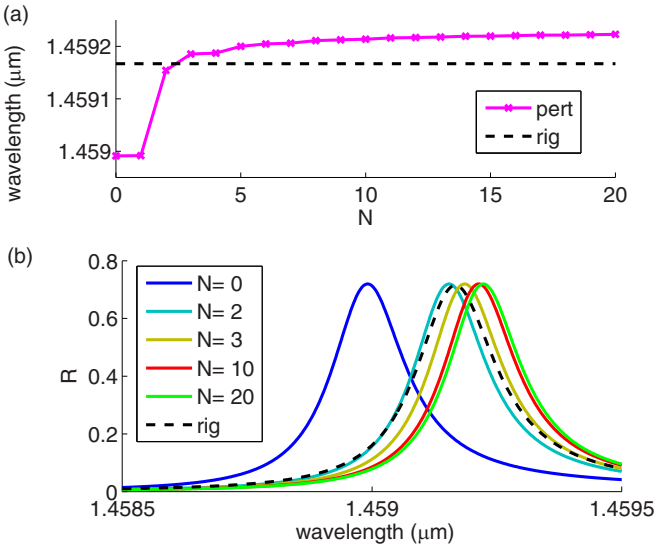

FIG. 6. Configuration 1—Convergence of the position of the resonance peak with respect to N. (a) Resonance wavelength calculated with the approached model with respect to N (solid line with stars) and calculated rigorously (dashed line). (b) Spectrum calculated with the approached model for various values of N (solid lines; the peak shifts towards upper wavelengths as N increases: blue for $N = 10$, cyan for $N = 2$, yellow for $N = 3$, red for $N = 10$, green for $N = 20$) and rigorously (dashed line).

We also considered a case where a TE mode is excited under conical incidence. We found that the resonance wavelength difference between the approached and rigorous calculations converges to one bandwidth over 6 (not shown).

B. Situation with two resonant orders

In the situation where two diffraction orders q and q' are resonant, the system given by Eq. (32) reduces to two coupled equations,

$$\begin{bmatrix} \frac{\lambda^2-\left(\lambda_q^{\text{pert}}\right)^2}{(\lambda_q)^2} & -(C_{q,q'}+\Sigma_{q,q'}) \\ -(C_{q',q}+\Sigma_{q',q}) & \frac{\lambda^2-\left(\lambda_{q'}^{\text{pert}}\right)^2}{(\lambda_{q'})^2} \end{bmatrix} \begin{pmatrix} \sigma_q \\ \sigma_{q'} \end{pmatrix} = \begin{pmatrix} C_{q,0} \\ C_{q',0} \end{pmatrix}, \tag{47}$$

where λ_q^{pert} and $\lambda_{q'}^{\text{pert}}$ are given by Eq. (42) and correspond to the eigenwavelengths of the modes q and q' when their mutual coupling is not taken into account. The eigenwavelengths of the studied structure are the wavelengths for which the determinant of the system of Eq. (47) is null. They are split on each side of the wavelength given by $\sqrt{[(\lambda_q^{\text{pert}})^2+(\lambda_{q'}^{\text{pert}})^2]/2}$, the splitting being governed by the coupling between the modes [antidiagonal terms in Eq. (47)], as already shown in [12,14,15,17].

In the particular case where the plane of incidence is a plane of symmetry of the structure (see Fig. 7), the two diffraction orders q and q' excite one guided mode of the reference structure, along two directions. Thus, the following relations are valid (both for TE modes and TM modes): $\lambda_q = \lambda_{q'}$, $C_{q,q'} = C_{q',q}$, $\Sigma_{q,q'} = \Sigma_{q',q}$, and $\Sigma_{q,q} = \Sigma_{q',q'}$. Moreover, in the case of a TE mode, we have $C^s_{q,0} = C^s_{q',0}$ and $C^p_{q,0} = -C^p_{q',0}$

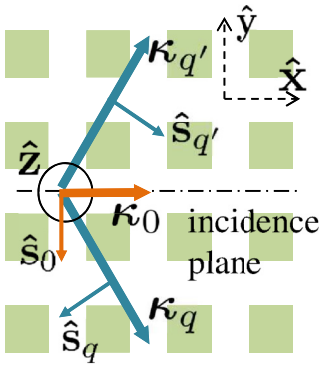

FIG. 7. Configuration where the plane of incidence is a plane of symmetry of the structure.

because $\hat{\mathbf{s}}_q$ and $\hat{\mathbf{s}}_{q'}$ are symmetrical with respect to the plane $(\hat{\mathbf{s}}_0,\hat{\mathbf{z}})$, and antisymmetrical with respect to the plane $(\hat{\boldsymbol{\kappa}}_0,\hat{\mathbf{z}})$ (see Fig. 7). In the same manner, for a TM mode, $C^s_{q,0} = -C^s_{q',0}$ and $C^p_{q,0} = C^p_{q',0}$.

The eigenwavelengths $\lambda^{\text{pert}}_{qq',\pm}$ of the two modes of the studied structure are given by $(\lambda^{\text{pert}}_{qq',\pm})^2 = (\lambda_q)^2[1 + \Sigma_{q,q} \pm (C_{q,q'} + \Sigma_{q,q'})]$. Note that in the particular case of normal incidence, we have $\Sigma_{q,q} = -\Sigma_{q,q'}$ for a TE mode and $\Sigma_{q,q} = \Sigma_{q,q'}$ for a TM mode, so that one of the eigenwavelengths is real, which corresponds to the antisymmetric mode which cannot be excited by a symmetric normal incident plane wave. Then, the coefficients σ_q and σ'_q are deduced from Eq. (47), $\sigma_q = \frac{[\lambda^2-(\lambda^{\text{pert}}_q)^2]C_{q,0}+(C_{q,q'}+\Sigma_{q,q'})C_{q',0}}{(\lambda_q)^2[\lambda^2-(\lambda^{\text{pert}}_{qq',+})^2][\lambda^2-(\lambda^{\text{pert}}_{qq',-})^2]}$, with a similar expression for σ'_q obtained by exchanging q and q'. From the relation between $C_{q,0}$ and $C_{q',0}$, we deduce that for a TE mode, $\sigma^s_q = \sigma^s_{q'}$ and $\sigma^p_q = -\sigma^p_{q'}$, and for a TM mode, $\sigma^s_q = -\sigma^s_{q'}$ and $\sigma^p_q = \sigma^p_{q'}$. Now, using the expression of $\mathbf{R}^{\text{pert}}_q$ [Eq. (38)], we obtain

$$\mathbf{R}^{\text{pert}}_q + \mathbf{R}^{\text{pert}}_{q'} = \begin{bmatrix} 2\sigma^s_q C^s_{0,q} & 0 \\ 0 & 2\sigma^p_q C^p_{0,q} \end{bmatrix}, \tag{48}$$

both for a TE mode and a TM mode. This means that the coupling between the two excited guided modes generates two hybrid modes, one of which is excited with a s polarization, while the other is excited with a p polarization, thus confirming the observations reported in the literature [19–22]. A full vectorial analysis was necessary to depict this phenomenon.

To validate our model in this case, we consider the configuration 2 involving a TE mode, a 2D grating, and oblique incidence. This second example is a 2D square grating illuminated under oblique incidence along one direction of periodicity (see Fig. 7). The structure is composed of a substrate with dielectric relative permittivity 2.25, a layer with thickness 400 nm and relative permittivity 4.0, and a 2D square grating with period 870 nm both along x and y axes, made with square holes with 300 nm width, 250 nm depth engraved in a material with relative permittivity 4.0. The angles of incidence are $\theta = 13°$ and $\phi = 0°$. In this configuration, a TE mode can be excited through the $(0, -1)$ and $(0, +1)$ diffraction orders around 1.53 μm. The simultaneous excitation of a guided mode in the two symmetrical directions generates two modes, one with a field symmetric and the other antisymmetric with respect to the (x,z) plane. As shown with the theoretical considerations at the beginning of this section, the symmetric mode can be excited with a p incident polarization, while the antisymmetric mode can be excited with a s polarization. The spectra calculated with the approached model for $N = 10$ (dashed lines, R and T), with the rigorous numerical method (solid lines, Rrig and Trig), and for the reference structure (dotted lines, Rref and Tref) are plotted in Fig. 8 for (a) a s incident polarization and (b) a p polarization. Again, the two peaks are well represented by the approached model, for the bandwidth, maximum, and minimum. They are shifted a little toward greater wavelengths with respect to the rigorous peak. The energy conservation is fulfilled.

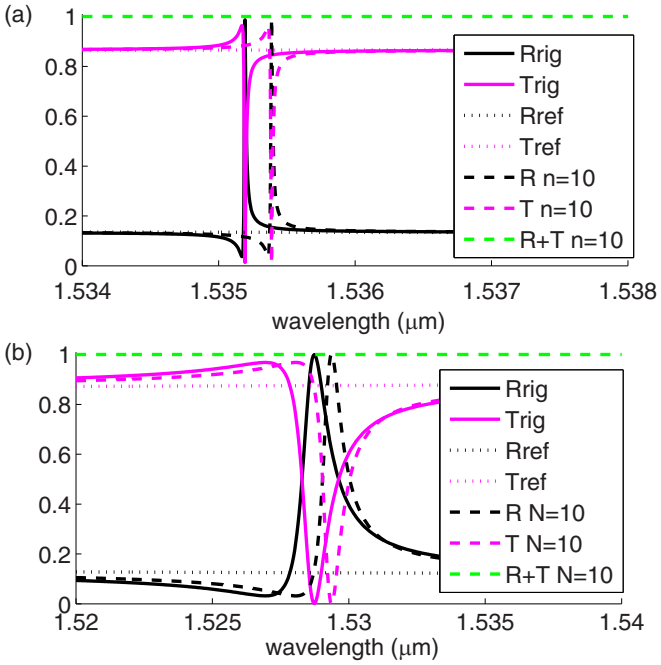

FIG. 8. Configuration 2—Reflectivity and transmittivity spectra calculated rigorously (straight lines, Rrig and Trig), with the approached method (dashed lines, R and T, and sum R+T) for $N = 10$, and for the reference structure (dotted lines, Rref and Tref). (a) For the s incident polarization, (b) for the p polarization.

Other examples of interest (see Appendix E) confirm the appropriateness and accuracy of the model.

V. CONCLUSION

A full vectorial approached model has been proposed to describe the reflectivity and transmittivity properties of guided-mode resonance gratings. We showed how the reflectivity (transmittivity) matrix can be expressed as the sum of a resonant and a nonresonant term. The nonresonant term is the reflectivity (transmittivity) matrix of a planar reference structure. The resonant term is a sum of matrices (one for each excited mode), with each matrix being expressed by coupling integrals involving the modes of the planar reference structure and the radiative modes. Our model is, of course, valid for the scalar configuration (typically a 1D grating illuminated along its direction of periodicity) and able to depict the physical behaviors already mentioned in the literature in this configuration.

Moreover, we demonstrated additional properties in the vectorial configuration (typically a 1D grating illuminated under conical incidence, or a 2D grating). A fundamental property of our resonant matrix is that one of its eigenvalues is null, with the other eigenvalue being resonant. The eigenvector associated with the non-null eigenvalue corresponds to the polarization for which the eigenmode is fully excited. Furthermore, writing the reflectivity (or transmittivity) matrix as the sum of a nonresonant and a resonant matrix allows the identification, in the polarization of the reflected (or transmitted) field, of the influence of the nonresonant field and that of the resonant field. We believe that this model provides a physical insight especially for configurations where the polarization of the modes is not trivial (not s or p polarization), and where the addition of the nonresonant and the resonant terms leads to a polarization that differs from the polarization expected from the excited mode alone.

We validated our model in various configurations (with TE or TM modes, one resonant or two resonant orders, 1D or 2D gratings) and showed a good robustness with respect to the grating depth (see the appendices).

Our model can be easily extended to configurations where several gratings are included inside the stack, and where the materials are anisotropic with z-axis symmetry. For bianisotropic materials, there is no technique to express the Green's tensor as two independent scalar Green's functions. One interesting further development of our method would be to consider configurations that are not periodic, as, for example, a coupling grating or a cavity resonator integrated grating filter (CRIGF, guided-mode resonance grating surrounded by Bragg reflectors) [35]. In this case, as the spatial frequencies in the Fourier space are no longer discrete but continuous, the problem cannot be expressed as a set of coupled equations, which requires further investigations.

APPENDIX A: THE VECTORIAL PROBLEM FOR A PLANAR STRUCTURE EXPRESSED AS TWO SCALAR PROBLEMS

The planar reference structure has a relative permittivity which is anisotropic with symmetry axis z. Thus, the diffraction or homogeneous vectorial problems associated with the reference problem can be divided into two scalar problems corresponding to the transverse electric and transverse magnetic cases (transverse with respect to the direction of propagation of the mode for the homogeneous problem and to the plane of incidence for the diffraction problem).

The equation satisfied by the electric field $\mathbf{E}_m^{\mathrm{ref}}(z)$ for the planar reference structure is [see Eq. (8)]

$$\bar{\bar{\mathbf{\Omega}}}_m\big(\mathbf{E}_m^{\mathrm{ref}}(z)\big) - k_0^2\bar{\bar{\boldsymbol{\epsilon}}}^{\mathrm{ref}}(z)\mathbf{E}_m^{\mathrm{ref}}(z) = \mathbf{0}, \tag{A1}$$

where the expression of the operator $\bar{\bar{\mathbf{\Omega}}}_m$ is given by Eq. (6).

To each diffraction order m with in-plane wave vector $\boldsymbol{\kappa}_m$, it is possible to associate an orthonormal basis $(\hat{\mathbf{s}}_m,\hat{\boldsymbol{\kappa}}_m,\hat{\mathbf{z}})$ (even for evanescent orders), where $\hat{\mathbf{s}}_m = \hat{\boldsymbol{\kappa}}_m \times \hat{\mathbf{z}}$. The operator $\bar{\bar{\mathbf{\Omega}}}_m$ can then be written as

$$\begin{aligned}\bar{\bar{\mathbf{\Omega}}}_m = {}& \big(\kappa_m^2 - \partial_z^2\big)\hat{\mathbf{s}}_m\hat{\mathbf{s}}_m - \partial_z^2\hat{\boldsymbol{\kappa}}_m\hat{\boldsymbol{\kappa}}_m + \kappa_m^2\hat{\mathbf{z}}\hat{\mathbf{z}} \\ & + i\kappa_m\partial_z(\hat{\mathbf{z}}\hat{\boldsymbol{\kappa}}_m + \hat{\boldsymbol{\kappa}}_m\hat{\mathbf{z}}).\end{aligned} \tag{A2}$$

In the following, for a given vector $\mathbf{V}$, the scalar quantities V_s, V_κ, and V_z will refer to the components on $\hat{\mathbf{s}}_m$, $\hat{\boldsymbol{\kappa}}_m$, and $\hat{\mathbf{z}}$ (respectively) of the vector $\mathbf{V}$.

Projecting Eq. (A1) on $\hat{\mathbf{s}}_m$ gives

$$\big[\partial_z^2 + (\gamma^o)^2\big]E_{m,s}^{\mathrm{ref}} = 0 \quad \text{with} \quad (\gamma^o)^2 = k_0^2\epsilon^o - \kappa_m^2, \tag{A3}$$

which corresponds to the transverse electric case.

The projections of Eq. (A1) on $\hat{\boldsymbol{\kappa}}_m$ and $\hat{\mathbf{z}}$ couple $E_{m,\kappa}^{\mathrm{ref}}$ and $E_{m,z}^{\mathrm{ref}}$,

$$\big(-\partial_z^2 - k_0^2\epsilon^o\big)E_{m,\kappa}^{\mathrm{ref}} + i\kappa_m\partial_z E_{m,z}^{\mathrm{ref}} = 0, \tag{A4}$$

$$\big(\kappa_m^2 - k_0^2\epsilon^e\big)E_{m,z}^{\mathrm{ref}} + i\kappa_m\partial_z E_{m,\kappa}^{\mathrm{ref}} = 0. \tag{A5}$$

Using the Maxwell equation $\boldsymbol{\nabla}\times\mathbf{E} = i\omega\mathbf{B}$, we can express the transverse magnetic field component $B_{m,s}^{\mathrm{ref}}$ with respect to $E_{m,\kappa}^{\mathrm{ref}}$ and $E_{m,z}^{\mathrm{ref}}$:

$$i\omega B_{m,s}^{\mathrm{ref}} = i\kappa_m E_{m,z}^{\mathrm{ref}} - \partial_z E_{m,\kappa}^{\mathrm{ref}}. \tag{A6}$$

Combining Eqs. (A4)–(A6), we obtain

$$\left[\partial_z\frac{1}{\epsilon^o}\partial_z + \frac{(\gamma^e)^2}{\epsilon^e}\right]B_{m,s}^{\mathrm{ref}} = 0 \quad \text{with} \quad (\gamma^e)^2 = k_0^2\epsilon^e - \kappa_m^2, \tag{A7}$$

which corresponds to the transverse magnetic case.

APPENDIX B: THE GREEN'S TENSOR EXPRESSED AS TWO SCALAR GREEN'S FUNCTIONS

The Green's tensor for the planar reference structure with a relative permittivity anisotropic with symmetry axis z can be expressed as two scalar Green's functions, also corresponding to the transverse electric and transverse magnetic cases. The Green's tensor is the solution of

$$\bar{\bar{\mathbf{\Omega}}}_m(\bar{\bar{\mathbf{G}}}_m(z,z')) - k_0^2\bar{\bar{\boldsymbol{\epsilon}}}^{\mathrm{ref}}(z)\bar{\bar{\mathbf{G}}}_m(z,z') = k_0^2\delta(z-z')\bar{\bar{\mathbf{I}}}. \tag{B1}$$

We note $G_m^{X,Y}$, the $\hat{\mathbf{X}}\hat{\mathbf{Y}}$ component of the Green's tensor (with $\hat{\mathbf{X}}$ and $\hat{\mathbf{Y}}$ being equal to $\hat{\mathbf{s}}_m$, $\hat{\boldsymbol{\kappa}}_m$ and $\hat{\mathbf{z}}$ successively). Using the expression of $\bar{\bar{\mathbf{\Omega}}}_m$ in the $(\hat{\mathbf{s}}_m,\hat{\boldsymbol{\kappa}}_m,\hat{\mathbf{z}})$ basis leads to several results.

First, it is possible to show that $G_m^{s,s}$ is the solution of

$$\big\{\partial_z^2 + [\gamma^o(z)]^2\big\}G_m^{s,s} = -k_0^2\delta(z-z'), \tag{B2}$$

which is the scalar equation for the transverse electric case. Second, we find that $G_m^{s,\kappa}$, $G_m^{s,z}$, $G_m^{\kappa,s}$, and $G_m^{z,s}$ are equal to zero. Third, $G_m^{\kappa,\kappa}$ and $G_m^{z,\kappa}$ are coupled by the following equations:

$$\big[-\partial_z^2 - k_0^2\epsilon^o(z)\big]G_m^{\kappa,\kappa} + i\kappa_m\partial_z G_m^{z,\kappa} = k_0^2\delta(z-z'), \tag{B3}$$

$$\big[\kappa_m^2 - k_0^2\epsilon^e(z)\big]G_m^{z,\kappa} + i\kappa_m\partial_z G_m^{\kappa,\kappa} = 0, \tag{B4}$$

while $G_m^{\kappa,z}$ and $G_m^{z,z}$ are coupled by

$$\big[-\partial_z^2 - k_0^2\epsilon^o(z)\big]G_m^{\kappa,z} + i\kappa_m\partial_z G_m^{z,z} = 0, \tag{B5}$$

$$\big[\kappa_m^2 - k_0^2\epsilon^e(z)\big]G_m^{z,z} + i\kappa_m\partial_z G_m^{\kappa,z} = k_0^2\delta(z-z'). \tag{B6}$$

Using Eqs. (B3) and (B4) and introducing

$$G_m^{p,\kappa} = i\kappa_m G_m^{z,\kappa} - \partial_z G_m^{\kappa,\kappa}, \tag{B7}$$

it is obtained that $G_m^{p,\kappa}$ is the solution of

$$\left\{\partial_z \frac{1}{\epsilon^o(z)}\partial_z + \frac{[\gamma^e(z)]^2}{\epsilon^e(z)}\right\} G_m^{p,\kappa} = \partial_z \frac{k_0^2}{\epsilon^o(z)}\delta(z-z'). \tag{B8}$$

From Eq. (B3), we express $G_m^{\kappa,\kappa}$ with respect to $G_m^{p,\kappa}$,

$$G_m^{\kappa,\kappa} = \frac{\partial_z G_m^{p,\kappa} - k_0^2\delta(z-z')}{k_0^2\epsilon^o(z)}. \tag{B9}$$

And from Eq. (B4), we express $G_m^{z,\kappa}$ with respect to $G_m^{p,\kappa}$,

$$G_m^{z,\kappa} = \frac{-i\kappa_m G_m^{p,\kappa}}{k_0^2\epsilon^e(z)}. \tag{B10}$$

Following the same steps, using Eqs. (B5) and (B6) and introducing

$$G_m^{p,z} = G_m^{z,z} - \frac{\partial_z G_m^{\kappa,z}}{i\kappa_m}, \tag{B11}$$

it is obtained that $G_m^{p,z}$ is the solution of

$$\left\{\partial_z \frac{1}{\epsilon^o(z)}\partial_z + \frac{[\gamma^e(z)]^2}{\epsilon^e(z)}\right\} G_m^{p,z} = -\frac{k_0^2}{\epsilon^e(z)}\delta(z-z'). \tag{B12}$$

From Eq. (B5), we express $G_m^{\kappa,z}$ with respect to $G_m^{p,z}$,

$$G_m^{\kappa,z} = i\kappa_m \frac{\partial_z G_m^{p,z}}{k_0^2\epsilon^o(z)}. \tag{B13}$$

And from Eq. (B6), we express $G_m^{z,z}$ with respect to $G_m^{p,z}$,

$$G_m^{z,z} = \frac{\kappa_m^2 G_m^{p,z} - k_0^2\delta(z-z')}{k_0^2\epsilon^e(z)}. \tag{B14}$$

The left side of Eqs. (B8) and (B12) is the operator involved in the equation for the transverse magnetic field problem [see Eq. (A7)]. Therefore, $G_m^{p,\kappa}$ and $G_m^{p,z}$ are two Green's functions, associated with the transverse magnetic field problem but with different sources [see the right side of Eqs. (B8) and (B12)]. In the following section, we deduce the link between $G_m^{p,\kappa}$ and $G_m^{p,z}$ from the reciprocity principle.

Note on the singularity of the Green's functions. From Eq. (B8), it appears that $\partial_z G_m^{p,\kappa}(z,z')$ presents a singularity equal to $k_0^2\delta(z-z')$, from which we deduce, using Eq. (B9), that $G_m^{\kappa,\kappa}$ does not have any singularity at the interface $z=z'$. It also appears that $G_m^{p,\kappa}$ is nonsingular, and from Eq. (B10) that $G_m^{z,\kappa}$ is also nonsingular. From Eq. (B12), it appears that $G_m^{p,z}$ and $\partial_z G_m^{p,z}(z,z')$ are nonsingular. From Eq. (B13), we deduce that $G_m^{\kappa,z}$ is nonsingular, while from Eq. (B14), $G_m^{z,z}$ presents a singularity equal to $-\delta(z-z')/\epsilon^e(z)$. To sum up, we can write the Green's tensor $\bar{\bar{\mathbf{G}}}_m(z,z')$ separating the nonsingular part $\bar{\bar{\mathbf{G}}}_m^{\mathrm{NS}}(z,z')$ and the singularity,

$$\bar{\bar{\mathbf{G}}}_m(z,z') = \bar{\bar{\mathbf{G}}}_m^{\mathrm{NS}}(z,z') - \frac{1}{\epsilon^e}\delta(z-z')\hat{\mathbf{z}}\hat{\mathbf{z}}. \tag{B15}$$

APPENDIX C: PROPERTIES OF THE GREEN'S FUNCTIONS RELATED TO THE RECIPROCITY PRINCIPLE

We consider a Hilbert function space with an Euclidian scalar product defined by $\langle f|g\rangle = \int_{-\infty}^{\infty} dz f(z)g(z)$. The operators $\mathcal{L}_s = \partial_z^2 + [\gamma^o(z)]^2$ and $\mathcal{L}_p = \partial_z \frac{1}{\epsilon^o(z)}\partial_z + \frac{[\gamma^e(z)]^2}{\epsilon^e(z)}$ on the left-hand side of Eqs. (B2), (B8), and (B12) are self-adjoint. Writing $\langle \mathcal{L}_s G_m^{s,s}|G_m^{s,s}\rangle = \langle G_m^{s,s}|\mathcal{L}_s G_m^{s,s}\rangle$ and using Eq. (B2), we deduce that

$$G_m^{s,s}(z,z') = G_m^{s,s}(z',z). \tag{C1}$$

Writing $\langle \mathcal{L}_p G_m^{p,z}|G_m^{p,z}\rangle = \langle G_m^{p,z}|\mathcal{L}_p G_m^{p,z}\rangle$ and using Eq. (B12), we also deduce that

$$\frac{G_m^{p,z}(z,z')}{\epsilon^e(z)} = \frac{G_m^{p,z}(z',z)}{\epsilon^e(z')}. \tag{C2}$$

Last, writing $\langle \mathcal{L}_p G_m^{p,z}|G_m^{p,\kappa}\rangle = \langle G_m^{p,z}|\mathcal{L}_p G_m^{p,\kappa}\rangle$ and using Eqs. (B8) and (B12), we deduce that

$$G_m^{p,\kappa}(z,z') = \frac{\epsilon^e(z)}{\epsilon^o(z')}\partial_{z'} G_m^{p,z}(z',z), \tag{C3}$$

which, in combination with Eq. (C2), leads to

$$G_m^{p,\kappa}(z,z') = \frac{\epsilon^e(z')}{\epsilon^o(z')}\partial_{z'} G_m^{p,z}(z,z'). \tag{C4}$$

These four relations are mathematical expressions for the consequences of the reciprocity principle on the Green's tensor, and they can be used to express $\bar{\bar{\mathbf{G}}}_m(z,z')$ with respect to $G_m^{s,s}$ and $G_m^{p,z}$ only.

APPENDIX D: EXPANSION OF THE GREEN'S TENSOR ON ITS EIGENMODES

Transverse electric Green's function. The equation satisfied for the Green's function $G_m^{s,s}$ (transverse electric case) is

$$\left[\partial_z^2 + \left(\frac{2\pi}{\lambda}\right)^2 \epsilon^o(z) - \kappa_m^2\right] G_m^{s,s} = -\left(\frac{2\pi}{\lambda}\right)^2 \delta(z-z'). \tag{D1}$$

The homogeneous equation [Eq. (A3)] for a mode with an electric field $\mathcal{E}^n(z)\hat{\mathbf{s}}_m$ and an eigenwavelength λ_n can be written as

$$\frac{1}{\sqrt{\epsilon^o}}\left(\partial_z^2 - \kappa_m^2\right)\frac{1}{\sqrt{\epsilon^o}}\left(\sqrt{\epsilon^o}\mathcal{E}^n\right) = -\left(\frac{2\pi}{\lambda_n}\right)^2 \left(\sqrt{\epsilon^o}\mathcal{E}^n\right). \tag{D2}$$

For the sake of simplicity, we do not specify the dependence of the wavelength λ_n and the field $\mathcal{E}^n(z)$ of the eigenmode on the subscript m related to the in-plane wave vector $\boldsymbol{\kappa}_m$ considered in Eq. (D1).

As $\frac{1}{\sqrt{\epsilon^o}}(\partial_z^2 - \kappa_m^2)\frac{1}{\sqrt{\epsilon^o}}$ is a self-adjoint operator, its eigenmodes form a basis and satisfy an orthogonality condition,

$$\int_{z=-\infty}^{z=+\infty} dz \epsilon^o(z)\mathcal{E}^n(z)\mathcal{E}^{n'}(z) = \delta_{n,n'}. \tag{D3}$$

We now want to expand $G_m^{s,s}$ on the basis formed by its eigenmodes,

$$G_m^{s,s}(z,z') = \sum_n f_n(z')\mathcal{E}^n(z). \tag{D4}$$

Inserting this expression into Eq. (D1) and using Eq. (D2), we obtain

$$\sum_n f_n(z')\left[\left(\frac{2\pi}{\lambda}\right)^2-\left(\frac{2\pi}{\lambda_n}\right)^2\right]\epsilon^o(z)\mathcal{E}^n(z) = -\left(\frac{2\pi}{\lambda}\right)^2\delta(z-z'), \tag{D5}$$

from which we deduce, using the orthogonality condition [Eq. (D3)],

$$f_{n'}(z')\left[\left(\frac{2\pi}{\lambda}\right)^2-\left(\frac{2\pi}{\lambda_{n'}}\right)^2\right] = -\left(\frac{2\pi}{\lambda}\right)^2\mathcal{E}^{n'}(z'). \tag{D6}$$

Hence, $G_m^{s,s}$ is expanded on the basis of its eigenmodes,

$$G_m^{s,s}(z,z') = \sum_n \frac{\mathcal{E}^n(z)\mathcal{E}^n(z')}{\left[\left(\frac{\lambda}{\lambda_n}\right)^2-1\right]}. \tag{D7}$$

Transverse magnetic Green's function. The Green's function $G_m^{p,z}$ (transverse magnetic case) is the solution of

$$\left\{\partial_z\frac{1}{\epsilon^o}\partial_z+\frac{1}{\epsilon^e}\left[\left(\frac{2\pi}{\lambda}\right)^2\epsilon^e-\kappa_m^2\right]\right\}G_m^{p,z} = -\frac{1}{\epsilon^e}\left(\frac{2\pi}{\lambda}\right)^2\delta(z-z'). \tag{D8}$$

The homogeneous equation for a mode with a magnetic field $\mathcal{B}^n(z)\hat{\mathbf{s}}_m$ and an eigenwavelength λ_n can be written as

$$\left[\partial_z\frac{1}{\epsilon^o}\partial_z-\frac{\kappa_m^2}{\epsilon^e}\right]\mathcal{B}^n = -\left(\frac{2\pi}{\lambda_n}\right)^2\mathcal{B}^n. \tag{D9}$$

As $[\partial_z\frac{1}{\epsilon^o}\partial_z-\frac{\kappa_m^2}{\epsilon^e}]$ is a self-adjoint operator, its eigenmodes form a basis and satisfy an orthogonality condition,

$$\int_{z=-\infty}^{z=+\infty} dz[c\mathcal{B}^n(z)][c\mathcal{B}^{n'}(z)] = \delta_{n,n'}, \tag{D10}$$

where the speed of light c in vacuum has been introduced so as to deal with quantities which have the unit of an electric field. Following the same steps as for the $G_m^{s,s}$ function leads to

$$G_m^{p,z}(z,z') = \sum_n \frac{c^2\mathcal{B}^n(z)\mathcal{B}^n(z')}{\left[\left(\frac{\lambda}{\lambda_n}\right)^2-1\right]\epsilon^e(z')}. \tag{D11}$$

Green's tensor. We will use the results of Appendix C to expand the Green's tensor on its eigenmodes. From Eq. (C3), one gets

$$G_m^{p,\kappa}(z,z') = c^2\sum_n \frac{\mathcal{B}^n(z)\partial_{z'}\mathcal{B}^n(z')}{\left[\left(\frac{\lambda}{\lambda_n}\right)^2-1\right]\epsilon^o(z')}. \tag{D12}$$

Then the equations relating $G_m^{z,z}$ and $G_m^{\kappa,z}$ to $G_m^{p,z}$ [Eqs. (B14) and (B13)] give

$$G_m^{z,z}(z,z') = c^2\sum_n \frac{1}{\left[\left(\frac{\lambda}{\lambda_n}\right)^2-1\right]}\left[\frac{\kappa_m\mathcal{B}^n(z)}{k_0\epsilon^e(z)}\right]\left[\frac{\kappa_m\mathcal{B}^n(z')}{k_0\epsilon^e(z')}\right] - \frac{1}{\epsilon^e}\delta(z-z')\hat{\mathbf{z}}\hat{\mathbf{z}}, \tag{D13}$$

and

$$G_m^{\kappa,z}(z,z') = c^2\sum_n \frac{1}{\left[\left(\frac{\lambda}{\lambda_n}\right)^2-1\right]}\left[\frac{i\partial_z\mathcal{B}^n(z)}{k_0\epsilon^o(z)}\right]\left[\frac{\kappa_m\mathcal{B}^n(z')}{k_0\epsilon^e(z')}\right]. \tag{D14}$$

Following the same steps, the equations relating $G_m^{z,\kappa}$ and $G_m^{\kappa,\kappa}$ to $G_m^{p,\kappa}$ [Eqs. (B10) and (B9)] give

$$G_m^{z,\kappa}(z,z') = -c^2\sum_n \frac{1}{\left[\left(\frac{\lambda}{\lambda_n}\right)^2-1\right]}\left[\frac{\kappa_m\mathcal{B}^n(z)}{k_0\epsilon^e(z)}\right]\left[\frac{i\partial_{z'}\mathcal{B}^n(z')}{k_0\epsilon^o(z')}\right], \tag{D15}$$

and

$$G_m^{\kappa,\kappa}(z,z') = -c^2\sum_n \frac{1}{\left[\left(\frac{\lambda}{\lambda_n}\right)^2-1\right]}\left[\frac{i\partial_z\mathcal{B}^n(z)}{k_0\epsilon^o(z)}\right]\left[\frac{i\partial_{z'}\mathcal{B}^n(z')}{k_0\epsilon^o(z')}\right]. \tag{D16}$$

To sum up, $\bar{\bar{\mathbf{G}}}_m^{\mathrm{NS}}$ can be written in the form

$$\bar{\bar{\mathbf{G}}}_m^{\mathrm{NS}}(z,z') = \sum_n \frac{\mathbf{A}_n(z)\otimes\overline{\mathbf{A}_n}(z')}{\left[\left(\frac{\lambda}{\lambda_n}\right)^2-1\right]}, \tag{D17}$$

where $\otimes$ denotes the tensor product between two vectors, $\mathbf{A}_n(z)$ is defined by

$$\mathbf{A}_n(z) = \mathcal{E}_n(z)\hat{\mathbf{s}}_m - ic\left[\frac{-\partial_z}{k_0\epsilon^o(z)}\hat{\boldsymbol{\kappa}}_m+\frac{i\kappa_m}{k_0\epsilon^e(z)}\hat{\mathbf{z}}\right]\mathcal{B}_n(z), \tag{D18}$$

while $\overline{\mathbf{A}_n}(z')$ is the complex conjugate of $\mathbf{A}_n(z')$. From the Maxwell equation $\boldsymbol{\nabla}\times\mathbf{H} = \frac{\partial\mathbf{D}}{\partial t}$, it is easy to show that $\mathbf{A}_n$ is the electric field of the mode.

APPENDIX E: SUPPLEMENTAL NUMERICAL VERIFICATIONS

1. Configuration 3: TM mode, 1D grating, quasinormal classical incidence

We now consider the quasinormal incidence case where a guided mode can be excited along two counterpropagative directions through two opposite diffraction orders. The grating is 1D and the plane of incidence is perpendicular to the grating grooves. The combination of the two modes gives one mode with a field symmetric and another with a field antisymmetric with respect to the plane normal to the direction of propagation of the modes. They correspond to the edges of a band gap in the dispersion relation of the structure. The symmetric mode is well excited with an incident plane wave and gives a broad peak, while the antisymmetric mode is scarcely excited, leading to a thin peak that disappears under normal incidence. The considered structure is the same as in that of configuration 1, the only difference being the incident field. The angles of incidence are set to $\theta = 0.01^\circ$ and $\phi = 0^\circ$. In this configuration, a TM guided mode is excited around 1.357 μm through the $(+1)$ and (-1) diffraction orders of the grating, and the resonances are observable for the p polarization.

We plot in Fig. 9(a) the spectrum calculated with the approached model for $N = 2$, $N = 20$, and rigorously. As

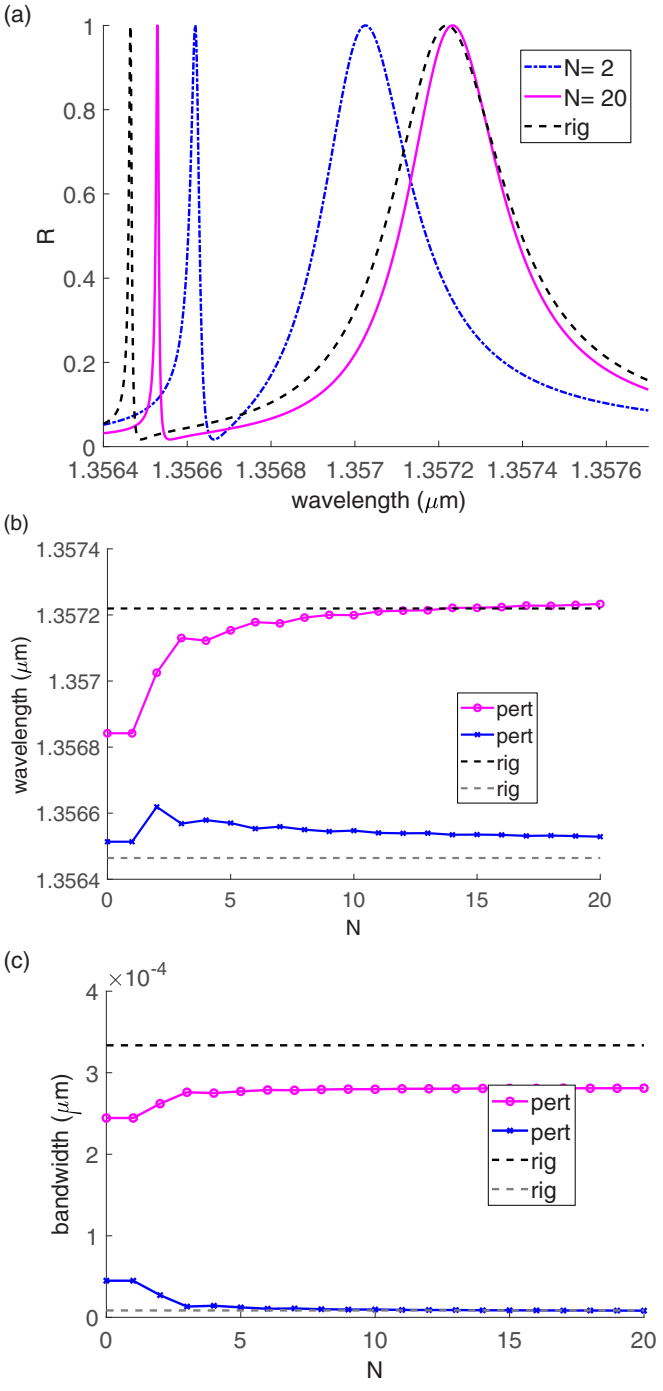

FIG. 9. Configuration 3—Convergence of the position of the resonance peaks with respect to N. (a) Spectrum calculated for p incident polarization for $N = 2$ (blue dash-dotted line), $N = 20$ (pink solid line), and rigorously (dashed line). (b) Resonance wavelength and (c) bandwidth of the two peaks calculated with the approached model with respect to N (solid lines) and calculated rigorously (dashed lines).

expected, we observe a broad and a thin peak. The approached calculation gives the right layout of the two peaks, with the broad peak for upper wavelengths and the thin peak for smaller wavelengths. Taking into account more $C_{q,n,q'}$ coefficients brings the approached calculation closer to the rigorous one. We have checked that the energy conservation (R+T = 1) is fulfilled also in this case (not shown on the curves).

The change of the resonance wavelength and bandwidth with respect to N can be seen in Figs. 9(b) and 9(c). The position of the two peaks is related to the coupling between the two counterpropagative modes: the higher the coupling, the greater the difference between the two resonance wavelengths. Hence, we observe in Fig. 9(b) that the distance between the two peaks increases with the number of coupling integrals, $C_{q,n,q'}$. The separation of the two peaks has an impact on the shape and, as a consequence, on the width of the peaks [see Fig. 9(c)].

We also considered a case where a TE mode is excited under quasinormal incidence (not shown here). The spectra obtained with the approached model are remarkably close to the rigorous results (closer than for the TM mode).

2. Configuration 4: TE mode, 1D grating, classical incidence—variation of the grating depth *h*

Our fourth example is a 1D grating illuminated under oblique classical incidence. The angles of incidence are set to $\theta = 30°$ and $\phi = 0°$. The structure is composed of a substrate with dielectric relative permittivity 2.25, a layer with thickness 250 nm and relative permittivity 4.0, and a 1D grating with period 742.2 nm and 442.2 nm groove width, engraved in a material with relative permittivity 4.0. We are interested in the resonance due to the excitation of a TE mode around 1.57 μm and to its evolution when the depth of the grating is varying.

We plot in Fig. 10 the centering wavelength [Fig. 10(a)] and the width [Fig. 10(b)] of the peak obtained with the

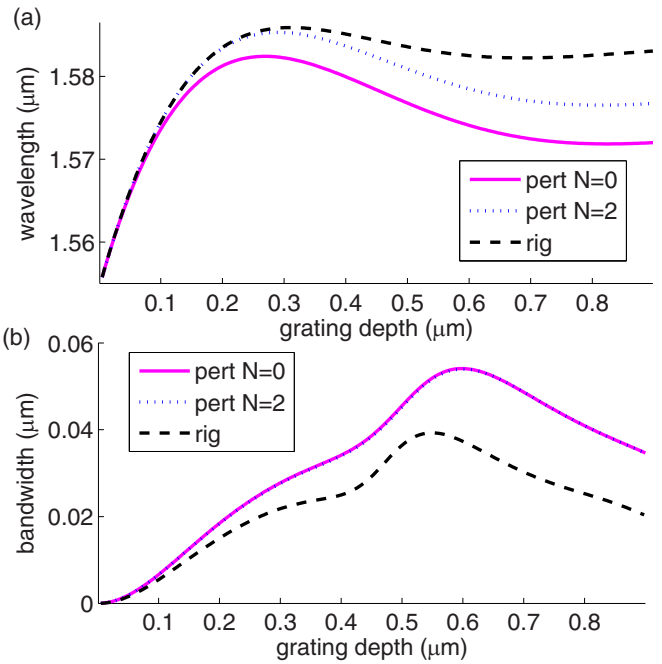

FIG. 10. (a) Configuration 4—Resonance wavelength calculated rigorously (dashed line) and with the approached method for $N = 0$ and $N = 2$ (solid pink and dashed blue lines). (b) Bandwidth calculated rigorously (dashed line) and with the approached method for $N = 0$ and $N = 2$ (solid pink and dashed blue lines).

rigorous numerical code and the approached method (for $N = 0$ and $N = 2$), with respect to the depth of the grating (from 0 to 1 μm). First, we observe that the global shape of the curves is similar for the rigorous and the approached methods: the resonance wavelength reaches a maximum for a grating depth around 300 nm, and the bandwidth for a grating depth between 500 and 600 nm. Second, the resonance wavelength is very well calculated with the approached method up to $\lambda/15$ for $N = 0$ and $\lambda/6$ for $N = 2$. It is all the more impressive that the relative permittivity of the material in which the grating is engraved is 4.0, which is not small. This relatively good robustness of the method concerning the resonance wavelength with respect to the grating depth may be attributed to the evanescent behavior of the mode in the grating layer. Last, we observe that the bandwidth is overestimated with the approached method and that increasing N does not improve the description of the bandwidth, as expected.

[1] A. B. Khanikaev, C. Wu, and G. Shvets, Fano-resonant metamaterials and their applications, Nanophotonics **2**, 247 (2013).

[2] M. Grande, M. A. Vincenti, T. Stomeo, G. V. Bianco, D. de Ceglia, N. Akozbek, V. Petruzzelli, G. Bruno, M. De Vittorio, M. Scalora, and A. D'Orazio, Graphene-based perfect optical absorbers harnessing guided mode resonances, Opt. Express **23**, 238453 (2015).

[3] G. Golubenko, A. Svakhin, V. Sychugov, A. Tischenko, E. Popov, and L. Mashev, Diffraction characteristics of planar corrugated waveguides, Opt. Quantum Electron. **18**, 123 (1986).

[4] S. Wang and R. Magnusson, Theory and applications of guided mode resonance filters, Appl. Opt. **32**, 2606 (1993).

[5] E. Popov, L. Mashew, and D. Maystre, Theoretical study of the anomalies of coated dielectric gratings, Opt. Acta **33**, 607 (1986).

[6] C. Sauvan, J. P. Hugonin, I. S. Maksymov, and P. Lalanne, Theory of the Spontaneous Optical Emission of Nanosize Photonic and Plasmonic Resonators, Phys. Rev. Lett. **110**, 237401 (2013).

[7] Q. Bai, M. Perrin, C. Sauvan, J.-P. Hugonin, and P. Lalanne, Efficient and intuitive method for the analysis of light scattering by a resonant nanostructure, Opt. Express **21**, 27371 (2013).

[8] C. Sauvan, J.-P. Hugonin, R. Carminati, and P. Lalanne, Modal representation of spatial coherence in dissipative and resonant photonic systems, Phys. Rev. A **89**, 043825 (2014).

[9] B. Vial, F. Zolla, A. Nicolet, and M. Commandré, Quasimodal expansion of electromagnetic fields in open two-dimensional structures, Phys. Rev. A **89**, 023829 (2014).

[10] V. Grigoriev, S. Varault, G. Boudarham, B. Stout, J. Wenger, and N. Bonod, Singular analysis of Fano resonances in plasmonic nanostructures, Phys. Rev. A **88**, 063805 (2013).

[11] J. Yang, H. Giessen, and P. Lalanne, Simple analytical expression for the peak-frequency shifts of plasmonic resonances for sensing, Nano Lett. **15**, 3439 (2015).

[12] S. M. Norton, T. Erdogan, and G. M. Morris, Coupled-mode theory of resonant-grating filters, J. Opt. Soc. Am. A **14**, 629 (1997).

[13] C. Blanchard, P. Viktorovitch, and X. Letartre, Perturbation approach for the control of the quality factor in photonic crystal membranes: Application to selective absorbers, Phys. Rev. A **90**, 033824 (2014).

[14] I. Evenor, E. Grinvald, F. Lenz, and S. Levit, Analysis of light scattering off photonic crystal slabs in terms of Feshbach resonances, Eur. Phys. J. D **66**, 231 (2012).

[15] P. Paddon and J. F. Young, Simple approach to coupling in textured planar waveguides, Opt. Lett. **23**, 1529 (1998).

[16] P. Paddon and J. F. Young, Two-dimensional vector-coupled-mode theory for textured planar waveguides, Phys. Rev. B **61**, 2090 (2000).

[17] F. Lemarchand, A. Sentenac, and H. Giovannini, Increasing the angular tolerance of resonant grating filters with doubly periodic structures, Opt. Lett. **23**, 1149 (1998).

[18] E. Sakat, S. Héron, P. Bouchon, G. Vincent, F. Pardo, S. Collin, J.-L. Pelouard, and R. Hadar, Metal-dielectric bi-atomic structure for angular-tolerant spectral filtering, Opt. Lett. **38**, 425 (2013).

[19] A. Mizutani, H. Kikuta, K. Nakalima, and K. Iwata, Nonpolarizing guided-mode resonant grating filter for oblique incidence, J. Opt. Soc. A **18**, 1261 (2001).

[20] A.-L. Fehrembach and A. Sentenac, Study of waveguide grating eigenmodes for unpolarized filtering applications, J. Opt. Soc. A **20**, 481 (2003).

[21] D. Lacour, G. Granet, J.-P. Plumey, and A. Mure-Ravaud, Polarization independence of a one-dimensional grating in conical mounting, J. Opt. Soc. Am. A **20**, 1546 (2003).

[22] G. Niederer, W. Nakagawa, and H. P. Herzig, Design and characterization of a tunable polarization-independent resonant grating filter, Opt. Express **13**, 2196 (2005).

[23] A. Monmayrant, S. Aouba, K. Chan Shin Yu, P. Arguel, A.-L. Fehrembach, A. Sentenac, and O. Gauthier-Lafaye, Experimental demonstration of 1D crossed gratings for polarization-independent high-Q filtering, Opt. Lett. **39**, 6038 (2014).

[24] T. Alaridhee, A. Ndao, M.-P. Bernal, E. Popov, A.-L. Fehrembach, and F. I. Baida, Transmission properties of slanted annular aperture arrays. Giant energy deviation over sub-wavelength distance, Opt. Express **23**, 11687 (2015).

[25] A.-L. Fehrembach, K. Sharshavina, F. Lemarchand, E. Popov, A. Monmayrant, P. Arguel, and O. Gauhtier-Lafaye, 2 × 1D crossed strongly modulated gratings for polarization independent tunable narrowband transmission filters, J. Opt. Soc. Am. A **34**, 234 (2017).

[26] A.-L. Fehrembach, D. Maystre, and A. Sentenac, Phenomenological theory of filtering by resonant dielectric gratings, J. Opt. Soc. Am. A **19**, 1136 (2002).

[27] B. Gralak and A. Tip, Macroscopic Maxwell's equations and negative index materials, J. Math. Phys. **51**, 052902 (2010).

[28] A. Yaghjian, Electric dyadic Green's functions in the source region, Proc. IEEE **68**, 248 (1980).

[29] M. Born and E. Wolf, *Principles of Optics* (Cambridge University Press, Cambridge, 1959).

[30] P. Lalanne and D. Lemercier-Lalanne, Depth dependence of the effective properties of subwavelength gratings, J. Opt. Soc. Am. A **4**, 450 (1997).

[31] M. Nevière, *The Homogeneous Problem, Electromagnetic Theory of Gratings*, edited by R. Petit (Springer Verlag, Berlin, 1980).

[32] S. Fan and J. D. Joannopoulos, Analysis of guided resonances in photonic crystal slabs, Phys. Rev. B **65**, 235112 (2002).

[33] L. Li, New formulation of the Fourier modal method for crossed surface-relief gratings, J. Opt. Soc. Am. A **14**, 2758 (1997).

[34] P. Chaumet, G. Demésy, O. Gauthier-Lafaye, A. Sentenac, E. Popov, and A.-L. Fehrembach, Electromagnetic modeling of large subwavelength-patterned highly resonant structures, Opt. Lett. **41**, 2358 (2016).

[35] S. Ura, J. Inoue, K. Kintaka, and Y. Awatsuji, Proposal of small-aperture guided-mode resonance filter, in *Proceedings of the 13th International Conference on Transparent Optical Networks (ICTON2011)* (IEEE, 2011).